TALLINNA TEHNIKAÜLIKOOL
TALLINN UNIVERSITY OF TECHNOLOGY

Department of Materials and Environmental Technology

MODIFICATION OF *P-N* JUNCTION OF COPPER-ZINC-TIN-SELENIDE MONOGRAIN LAYER SOLAR CELLS

VASK-TSINK-TINA-SELENIID MONOTERAMEMBRAAN-PÄIKESEPATAREI P-N ÜLEMINEKU MODIFITSEERIMINE

MASTER THESIS

KANG ZHONG
156307KAYM

Supervisor: Dr. Mare Altosaar
Senior Research Scientist
Laboratory of Photovoltaic Materials

Co-supervisor: Dr. Liina Reichmann
Engineer
Laboratory of Photovoltaic Materials

Materials and Processes of Sustainable Energetics
Tallinn, 2017

AUTHOR’S DECLARATION

Hereby I declare, that I have written this thesis independently.
No academic degree has been applied for based on this material.
All works, major viewpoints and data of the other authors used in this thesis have been referenced.

“.......” .... 2017..

Author: ....
/signature /

Thesis is in accordance with terms and requirements

“.......” .... 2017….

Supervisor: …..........................
/signature/

Accepted for defence

“.......”....................2017… .

Chairman of theses defence commission: ....
/name and signature/

CONTENTS

List of Abbreviations and symbols

ALD - Atomic layer deposition
Al_2O_3 – Aluminum oxide
Br_2-MeOH - Bromine in methanol
CZTSSe - $Cu_2ZnSn(SSe)_4$- copper zinc tin sulfide selenide
CZTSe - $Cu_2ZnSnSe_4$ – copper zinc tin selenide
CZTS - Cu_2ZnSnS_4 – copper zinc tin sulfide
CIGS - $Cu(InGa)Se_2$ - copper indium-gallium selenide
CIGSSe - $Cu(InGa)(SSe)_2$ - copper indium gallium sulfide selenide
CBD - Chemical solution deposition, Chemical Bath Deposition
c-Si - crystalline silicon
DI - Deionized water
EDX - Energy-dispersive X-ray spectroscopy
FF - Fill factor
HCL - Hydrochloric acid
H_2SO_4 - Sulfuric acid
I-V - Current-voltage
In_2S_3 – Indium selfide
J_{SC} - Short circuit current density
KI - Potassium iodide
KCN - Potassium cyanide
KOH - Potassium hydroxide
MGL - Monograin layer solar cell
η - Solar cell efficiency
PL - Photoluminescence
PLD - Pulsed laser deposition
PV - Photovoltaic
SEM - Scanning electron microscopy
SILAR - Successive ionic layer adsorption reaction
TU - Thiourea
TAA - Thioacetamide
V_{OC} - Open circuit voltage

1. INTRODUCTION

As we all know, with the development of science and technology, the demand for traditional energy sources such as fossil fuel is increasing every year, it leads to some bad influence for environment, such as air pollution and ecological destruction. It has challenged human survival and economic development. Currently, we human beings have to use more renewable energy to substitute traditional energy to solve this problem. There are quite a lot of sustainable energies, such as solar energy, wind energy, geothermal energy and tide energy etc.

Solar energy as an inexhaustible green energy has so many advantages, such as great energy reserves, widely distributed and clean. Nowadays, the current record energy conversion efficiency of - copper zinc tin sulfide selenide (CZTSSe)-based solar cells is around 12.6% [1], while the chalcopyrite compounds (copper indium gallium selenide ($Cu(In,Ga)Se_2$)) have higher efficiency around 21.7% [2]. Nevertheless, due to CZTSSe absorber material's special crystal structure, currently it's an ideal candidate to substitute $Cu(In,Ga)(S,Se)_2$ (CIGS) *p*-type material which is already at industrial production stage [4] in photovoltaic devices [3]. CZTSe (kesterite structured compound semiconductor) now has drawn a lot attention from scientists all over the world. As these compounds have so many advantages, like non-toxic, earth abundant and less consumed raw materials, high theoretical conversion efficiency, high absorption coefficient ($>10^4 cm^{-1}$), also optical band gap (1eV) [5] optimizing with the spectrum of solar cell etc.

However, the most widely used composition of CZTSe photovoltaic-grade absorber layer is not stoichiometric, Zn-rich and Cu-poor compositions [4], have shown the best devices: Cu/(Zn+Sn) ratio is between 0.7-0.9 and Zn/Sn is 1.1-1.25 [6]. Sometimes this off-stoichiometric initial composition leads to the formation of secondary phases, mostly ZnSe is found [7]. The existence of secondary phases in absorber material is still a big problem for the development of CZTSe solar cells [4]. Also, the problem how to build up a perfect formation of *p-n* junction to improve the electrical parameters and thus to improve the performance of solar cell, is a big issue.

So, the aim of this work is to try to find out: 1) the optimal heat-treatment conditions after CdS deposition by modification of heat-treatment temperature and heat-treatment time in different ambient conditions (closed vacuum, continuous vacuum pumping, air) for improvement the performance of CZTSe solar cells; 2) the best annealing conditions for the CZTSe absorber material by using different Se vapor pressures and different temperatures;

3) which are the optimal etching conditions after heat-treatment of absorber material; 4) if the intermediate layers (In_2S_3, Al_2O_3) have some good influence to the performance of CZTSe-based solar cells.

2. LITERATURE REVIEW AND THE OBJECTIVE OF STUDY

2.1. Photovoltaic solar cell

A solar cell or photovoltaic cell is an electrical device that can convert the energy of light into electricity directly by using semiconducting materials which have photovoltaic (PV) effect; it is physical, photo-chemical and photo-electrochemical phenomenon. Usually, we call photovoltaic system as solar panel. Photovoltaics are the most widely used method for producing electricity by using solar panels to convert sun energy into a flow of electrons. The photovoltaic effect means that photons of light exciting electrons in a light absorbing semiconductor material into a higher state of energy, allowing them to be carriers of electric current. It was first observed by Alexandre-Edmond Becquerel in 1839 [8-9].

2.1.1. Development of photovoltaic solar cell

There are several PV systems operating, but scientists are aimed to fabricate a high efficiency and low-cost solar cell instead of using traditional energy resources.

First-generation solar cell technology is mainly based on silicon, it includes single-crystalline (c-Si) and polycrystalline silicon PV cells. Polycrystalline silicon was used in an attempt to cut manufacturing costs, although the resulting cells are not as efficient as these based on single crystalline silicon [10]. c-Si PV technology is the most efficient of all PV technologies coverting absorbed sunlight into electricity with average efficiency of 16% to 20%. However the current cost of c-Si technology is still too expensive for widespread use, as the purifying process is too expensive and the reduction of the silicon wafer process also costs a lot. There are two ways to reduce the costs: (1) incorporate light trapping in the cell structure. (2) improve the surface passivation and the bulk passivation [10].

Second-generation solar cell technology is thin-film solar cells. However, they also aim to reach to some efficiency, but the materials used are quite cheaper than silicon, so it is cost effective. Thin-film solar cells can be made from a variety of materials, including amorphous silicon (which has no crystalline structure), gallium arsenide, copper indium diselenide ($CuInSe_2$, CIS), copper indium gallium sulfide selenide (CIGSSe) and cadmium telluride (CdTe) [11].

2.1.2. Working principle of photovoltaic solar cell

Diffusion between *p-n* junction. When *p*-type and *n*-type materials are contacted, then, due to the concentration gradient of electrons and holes in two different type materials, diffusion occurs in the vicinity of the surface between them. *n*-type is full of electrons, *p*-type is full of holes. Electrons start to diffuse from *n*-type to *p*-type. At the same time, holes diffuse from *p*-type region to *n*-type region. This diffusion creates an electron-hole free region in a very short distance at the interface region. This thin layer is called depletion region.

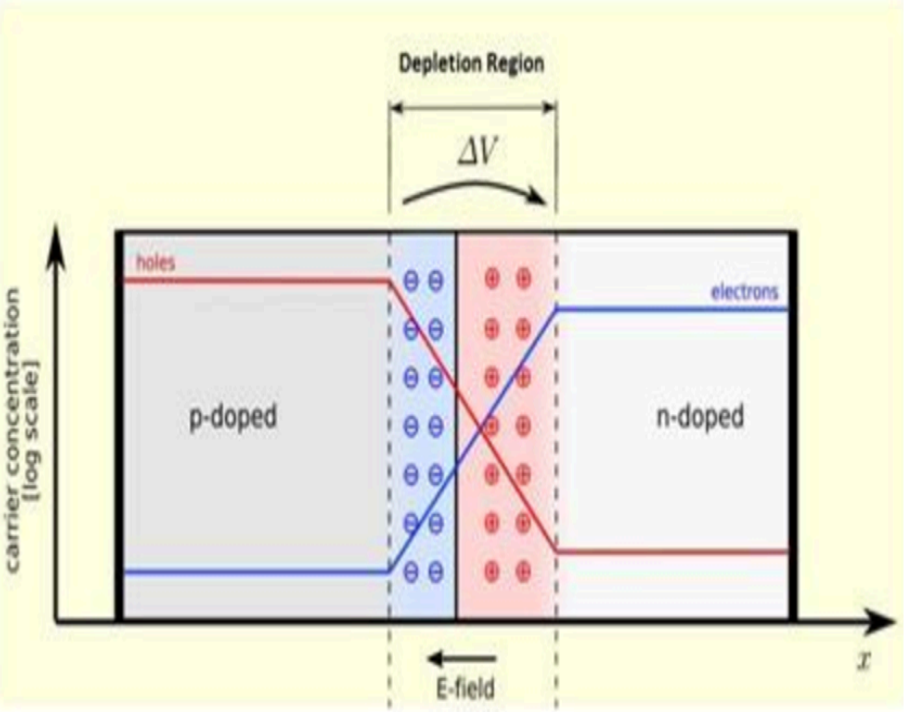

Figure 1. Majority carrier diffusion in p-n junction [12].

We can see it in Figure 1, blue line marks the electron concentration while red line indicates hole concentration through contact area of these semiconductor materials. There forms an electric field inside the depletion region from the *n*-side to the *p*-side. The electric field has a force to negative charges (electrons) entering the depletion region. Electrons generated by sun light near the depletion region in *p-type* material can pass to the *n*-side of the junction very easily [12]. When solar cell is connected into outer circuit, current flow occurs.

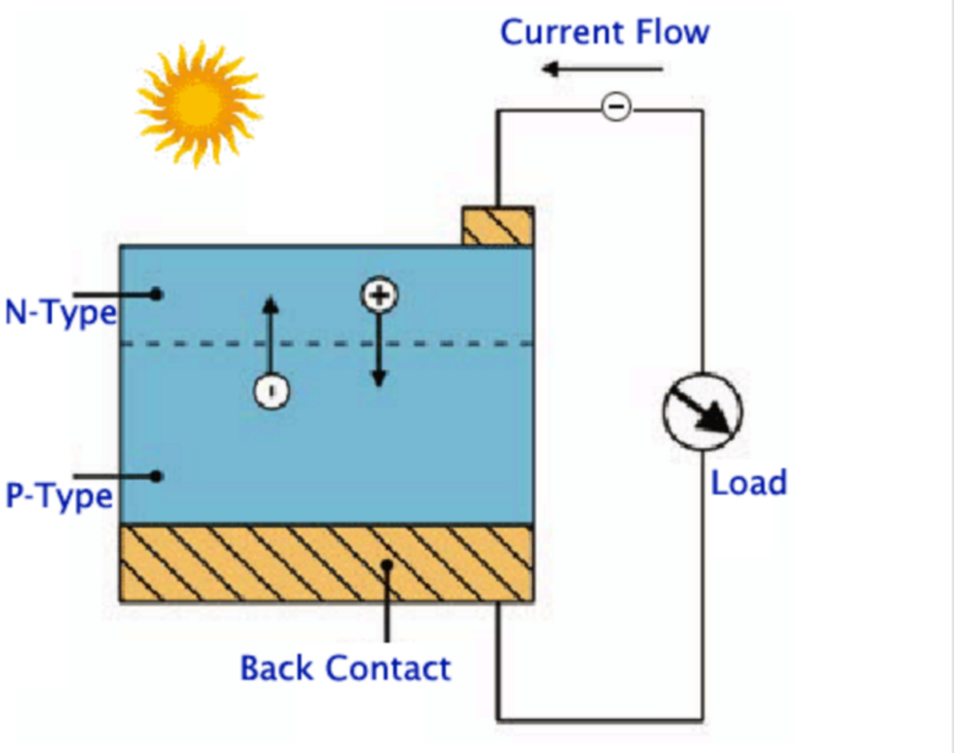

Figure 2. Photovoltaic solar cell generates electricity [13].

We can see in Figure 2, that if the metal contacts connect the *n*-type and *p*-type region with wires, then the electrons flow through this external load, so we need an external energy (solar irradiation) to create this current: that can push the electrons from *p*-type region into depletion region [12].

2.2. Monograin layer solar cell

2.2.1. Description of monograin layer solar cell

The monograin layer (MGL) solar cell consists of a one grain thick layer of crystals of monograin powder embedded into epoxy. This membrane works as light absorber. MGL has high photo-electronic parameters of single crystals [14]. MGL solar cell has many advantages: (1) low cost and simple technology of materials and devices (run-to-run technology can be used for membrane making); (2) the possibility of making flexible devices; (3) the possibility of using materials up to 100% [15]. However, it has some disadvantages: 1) only part of the membrane area (about 75 %) is working actively, because of epoxy between the crystals, 2) some designs need powder grains of nearly equal size and perfect monocrystalline structure; 3) there are problems (after synthesis the crystals' surface were not clean, it needs many steps like chemical etching and thermal annealing treatment to clean the crystals' surface) of surface preparation of the grains in the MGL [15].

2.2.2. Structure of monograin layer solar cell

Copper zinc tin-sulfide selenide (CZTSSe) monograin materials can be used as absorber materials in MGL solar cells due to their high absorption coefficient ($>10^4 cm^{-1}$) and suitable optical band gap (1-1.5eV) fitting well with the solar spectrum [5].

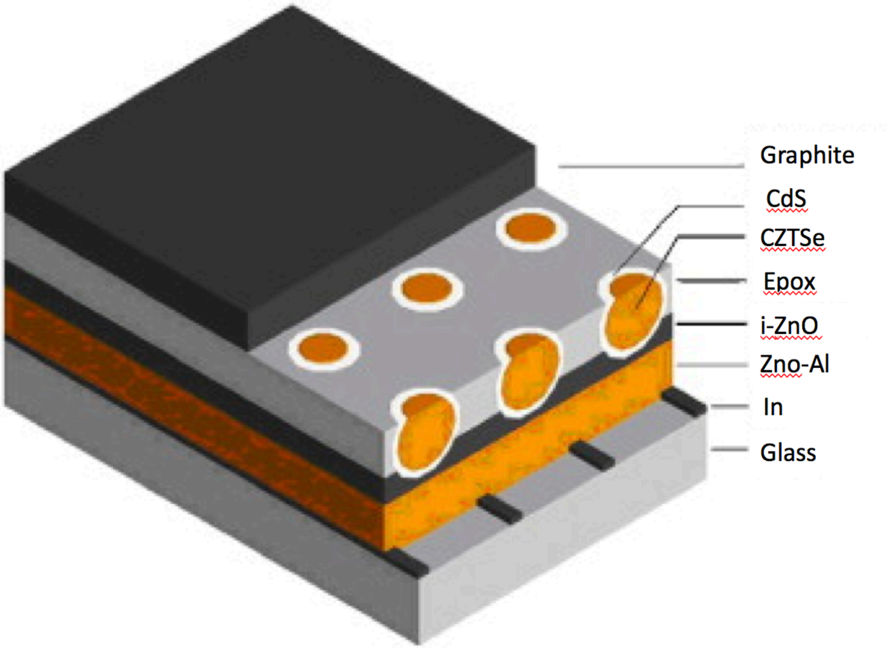

Figure 3. The device structure of CZTSe MGL solar cell: graphite back contact/CZTSe absorber/CdS buffer/i-ZnO/ZnO:Al window layer/glass (or flexible) substrate [16].

Monograin membranes are covered with the other necessary layers shown in the Figure 3 and then glued onto glass (or flexible) substrates.

2.3. Materials and methods used for making *p-n* junction

2.3.1. Basic characteristics of CZTSe absorber material

Recently, kesterite-structured copper zinc tin chalcogenide (sulfide/selenide) materials have drawn great attention to scientists, as they have great potential to substitute CIGSSe material because of the earth abundant constituent elements and lower cost [17]. A recent report about thin film solar cells shows that if to increase the content of Se in CZTSSe material, it will be easier for gaining *p*-type doping [18]. So, based on this report, we can expect higher results from higher Se content in CZTSSe thin film solar cells. The crystallization of electrodeposited CZTSe material in thin films started from 400°C and ended at 500°C, while crystal growth continued at higher temperatures. In order to increase crystallinity and enhance poor physical properties, CZTSe thin films annealed at 550°C exhibited the best and most-stable device performances, reaching up to 8.0 % active efficiency [19].

2.3.2. CdS buffer material

In the past few years, the deposition and characterization of cadmium sulfide semiconducting thin films has drawn great interest from scientists, as it has huge potential for the application in the area of fabrication electronic and optoelectronic devices [20]. It is reported that the kesterite absorber layer with CdS buffer layer is the key factor for improving the performance of solar cell, by using nitride source of cadmium sulfide, the light-dependent defect (long wavelength monochromatic illumination) of $Cu_2ZnSnSe_4$/CdS heterojunction solar cells can be eliminated, and these improvements lead to a decrease in series resistance and an increase in fill factor and increase power conversion efficiency from 7.0% to 8.2% [21]. Usually, in order to avoid the shunt paths, we use high resistivity cadmium sulfide as buffer material in photovoltaic devices [22]. CdS is widely used as buffer layer in solar cell structures as it has quite so many advantages: Reasonable conversion efficiency, stability and availability of low-cost deposition technique, intermediate band-gap (2.4 eV), high transparency, electron affinity, easy making of ohmic contact and finally the structure [23].

2.3.3. In_2S_3 as buffer or intermediate layer

Indium sulfide is an indium chalcogenide, it is III–VI semiconductor compound [24], and it is very important for the research work of photoelectric and photovoltaic (PV) applications [25]. It has stable chemical composition, photoconductivity, and luminescent characteristics at ambient conditions. It is used as an *n*-type semiconductor with an optical bandgap of 2.1-2.3 eV [26]. In_2S_3 has been viewed as a promising low-toxic buffer (or window) material, and has proven to improve the performance of the solar panels, at the same time reducing toxicity [27].

2.3.4. Intermediate layer of Al_2O_3

The idea of using Al_2O_3 in MGL solar cell stems from the silicon (Si) PV-industry, where rear surface passivation layers are used to boost the open-circuit voltage and so to improve the solar cells efficiency. It is proved that by reducing the surface and bulk recombination rates (passivation) the solar cell efficiency can be improved up to 30% by using Al_2O_3 layer in CIGS thin film solar cells [28-29].

2.3.5. Chemical etching

Monograin growth in molten fluxes results in homogeneous composition of the CZTSe powder material [30]. At synthesis temperature (>690°C) the used molten flux (KI, NaI) is saturated with the components used for synthesis of CZTSe. In the cooling process after synthesis-growth these dissolved components precipitate onto surfaces of CZTSe crystals. Sn(S,Se) secondary phases are low-band gap phases with the *Eg* around 1eV (this value was reported for a 1:1 stoichiometry compound; compounds with the other stoichiometry have band gaps between 1.1 and 2.5 eV), so if these phases are stayed at the surface of CZTSSe/CdS interface, the open circuit voltage value will decrease, then the whole performance of the solar cell will decrease [31]. So, the control of the secondary phases is one of most important issue for improving CZTSSe–based solar cell's performance [31]. Therefore we use always several etchants (Br_2-MeOH, HCl, KCN) to purify the surface of the crystals. It has been shown in [32] that Sn and Se were removed by HCl etching. Cu, Sn and Se were mainly dissolved in 10% KCN, and after 1% Br_2-MeOH etching, the material surfaces were Se-rich [32]. As the chemical etchants have selective influence, the crystals' surface structure needs healing after etching. It is made by heat-treatments. The prepared powders are used as absorber layers in MGL solar cells. Before CdS deposition, some another chemical treatment can lead to the best parameters of $Cu_2ZnSn(S,Se)_4$ monograin layer solar cells. So far, the best achieved CZTSe MGL solar cell efficiencies were about 4% [33]. As for CZTS material, it was shown in [34] that after bromine etching, elemental sulfur, Sn–O and/or Sn–Br species were formed on the CZTS crystal surfaces. Then, applying KCN etching, sulfur was completely removed, but oxides and bromides had been remained on the surface before CdS deposition. These species could influence the properties of deposited CdS. The absorber material crystals surface composition can be changed by different etching processes before CdS deposition, and improve the efficiency of MGL solar cell [31]. The best achieved and certified CZTSSe monograin layer solar cell efficiency is currently 9.5% (material's power conversion efficiency about 13%), information from private communication with colleagues from "crystalsol OÜ". Besides, there is a research work showing that the low temperature post-deposition annealing with surface etching is good for improving CZTSe-based solar cell's performance. After removing the secondary phase ZnSe by oxidizing etching, followed by annealing at 200°C, the solar cell's efficiency increased from 3% to 8.3% [36]. It can be understandable due to the changes in surface composition which leads to great improvement of the CdS/CZTSe heterojunction [36]. In [37] it was approved that the secondary phases can be removed by the etchant HCl and Br_2-MeOH, the absorber material was analyzed before and after chemical etching by some physical analyzing methods, such as scanning electron microscopy or photoluminescence, then the solar cell was tested by *I-V* curve measurement, the results show that the Cu, Sn related phase ($Cu_2Sn(S,Se)_3$) can reduce the open circuit voltage and fill factor values, decreasing the overall performance of solar cell. It was observed that all the parameters of the solar cell were improved by HCl etching, while Br_2-MeOH etching improved only fill factor and open circuit voltage values [37]. The best CZTSe solar cell performance is reported for the absorber materials synthesized under Cu-poor ([Cu]/([Sn]+[Zn]) ~ [0.7-0.95]) and Zn-rich ([Zn]/[Sn] ~ [1.0-1.25]) conditions. Sn-rich ([Zn]/[Sn]< 1) and Cu-rich ([Cu]/(Sn)+[Zn])> 1) conditions enhance the formation of low band gap Sn(S,Se) or $Cu_2Sn(S,Se)_3$ secondary phases and degenerated *p*-type $Cu_x(S,Se)$ leading to the decreased performance of the solar cells [37].

2.3.6. Influence of thermal treatment of CZTSe in Se vapor to the MGL solar cell parameters

Hahn and Schulze have successfully grown CZTSe single crystals for the first time [38]. Guen [39] found that CZTSe single crystals grown by gradient freezing of the melt, had *p*-type conductivity. Altosaar and her research group prepared solar cells using CZTSe monograin powder as absorber material and reported MGL solar cell open circuit voltage of 401 mV, short-circuit current density of 12 mA cm^{-2}, fill factor of 0.38 and efficiency of 1.8% [40]. However, these MGLs always contain secondary phases, so the solar cells have bad performance. In order to find out the importance of this quaternary semiconductor as a potential absorber layer, studies on CZTSe thin films grown by co-evaporation have been taken up by scientists. The studies show that the optimum substrate temperature to get the single-phase CZTSe films is 623 K, without annealing [41].

2.4. Deposition methods for buffer layer

2.4.1. Different deposition methods

There are reported several methods for buffer layer deposition, such as sputtering, pulse laser evaporation, physical vapor deposition, electrodeposition, screen printing, spray pyrolysis, metal organic vapor phase epitaxy (MOVPE)/metal organic chemical vapor deposition (MOCVD), successive ionic layer adsorption reaction (SILAR), molecular beam epitaxy and chemical bath deposition (CBD) [42]. Among all the methods, CBD is one of the most promising method for photovoltaic applications as it has so many advantages, such as high efficiency, cost effective and suitability for depositing large areas with high quality thin films. Always, this method involves slow release of sulfide ions via the controlled hydrolysis of thiourea into alkaline solution in the presence of cadmium salts [43]. In the laboratory, chemical bath deposition is the most widely used method for buffer layer deposition. In the frame of my thesis, I used only this method.

2.4.2. Chemical solution deposition

It is a method for depositing nanomaterials or thin films onto the membranes or other substrates. In 1960s, soviet scientists S.G. Mokrushin and Y.D. Tkachev were the first who tried this method for preparing CdS thin films [44]. Chemical solution deposition, also called chemical bath deposition (CBD) has proven to be the most suitable method to produce CdS films for photovoltaic applications, because this technique offers the following advantages [45]:

- an easy and continuous coverage on rough surfaces at minimal thicknesses;
- CBD does not require sophisticated instrumentation and expensive equipments;
- the starting chemicals are commonly available and cheap;
- a large number of substrates can be coated in a single run with proper design;
- electrical conductivity of the substrate is not the necessary requirement;
- chemical deposition results in pin hole free and uniform layers since the basic building blockes are ions instead of atoms.

Chemical solution deposition process involves two steps: nucleation and particle growth, where the ions of the bath solution are deposit onto solid surfaces. First of all, there should be worked out a procedure of making chemical bath solution, then after putting a substrate into the solution control the deposition by temperature, pH, concentrations of ions in the bath solution and time of the process [46]. However, the chemical deposition process has a big disadvantage - it generates some toxic waste [47]. The process of this method can be described by following chemical equations:

$$Cd^{2+} + 4NH_3 \Leftrightarrow Cd(NH_3)_4^{2+} \qquad (1)$$

$$\beta = [Cd(NH_3)_4^{2+}] / [Cd^{2+}][NH_3]_4 \qquad (2)$$

$$Cd^{2+}+2OH^- \Leftrightarrow Cd(OH)_2 \qquad (3)$$

$$SC(NH_2)_2 + 2OH^- \Leftrightarrow S^{2-} + 2H_2O + H_2CN_2 \qquad (4)$$

$$Cd(OH)_2 + S^{2-} \Leftrightarrow CdS + 2OH^- \qquad (5)$$

Ammonium hydroxide is used to provide the ammine ligand that forms tetra-ammine complex with Cd^{2+} (1). Stability constant of the tetra-ammine complex β can be written as equation (2). $Cd(NH_3)_4^{2+}$ provides Cd^{2+} ions into the solution slowly, allowing to regulate the rate of CdS deposition. Cd^{2+} will combine with OH^- ions and became $Cd(OH)_2$, thiourea provides S^{2-} into the solution, then $Cd(OH)_2$ will absorb S^{2-} and CdS will be deposited at the surface of the membranes. From the chemical equilibrium equation, we can calculate how much different ions we need, if the concentrations of ions of the equations left side is more, then the chemical reaction will go to the right direction. Otherwise, it will go to the left direction [48].

2.5. Summary of the literature review and the objective of study

Kesterite-structured copper zinc tin sulfide-selenide materials have drown great attention to scientists recently, as containing low cost, non-toxic and earth abundant elements. Also, they have high theoretical conversion efficiency, high absorption coefficient ($>10^4 cm^{-1}$) and optical band gap (1eV) optimizing with the spectrum of solar cell etc. There are lots of ways to optimize the performance of the solar cell, such as using different absorber materials with different deviations from stoichiometry, we can anneal them at different temperatures and in different element vapors, sometimes the intermediate layers (such as Al_2O_3 or In_2S_3) will have some good influence for increasing the performance of the solar cell. And some scientists also use different buffer layers to see how they influence to the properties of solar cells. Also, by using different chemical etching methods the surface composition of the absorber materials can be changed having good or bad influence to solar cell working ability.

My focus in this research work is to try to find out:

1. the optimal heat-treatment conditions after CdS deposition by modification of heat-treatment temperature and heat-treatment time in different ambient atmospheres (closed vacuum, continuous vacuum pumping, air) for as-grown material;
2. the best annealing conditions of the absorber material by changing different Se vapor pressures and different temperatures;
3. the optimal etching conditions for improving the performance of CZTSe solar cell;
4. if the intermediate layers (In_2S_3, Al_2O_3) have some good influence for the performance of CZTSe-based solar cells.

3. EXPERIMENTAL

3.1. Physical analysis methods used in the present study

3.1.1. Raman spectroscopy

Raman spectroscopy is a spectroscopic technique based on inelastic scattering of monochromatic light, usually from a laser source. When light is scattered from a molecule most photons are elastically scattered. The scattered photons have the same energy (frequency) and, therefore, wavelength, as the incident photons. However, a small fraction of light (approximately 1 in 10^7 photons) is scattered at optical frequencies different from, and usually lower than, the frequency of the incident photons. The process leading to this inelastic scatter is the termed Raman effect. Raman scattering can occur with a change in vibrational, rotational or electronic energy of a molecule. Chemists are concerned primarily with the vibrational Raman effect.The difference in energy between the incident photon and the Raman scattered photon is equal to the energy of a vibration of the scattering molecule. A plot of intensity of scattered light versus energy difference is a Raman spectrum. Raman spectroscopy is used for identification of chemical molecules [49]. The laser light interacts with molecular vibrations, phonons or other excitations in the system, then the energy of the laser photons is being shifted up or down. Finally, we can get the information from the shift in energy about the vibrational modes in the system [50].

3.1.2. Scanning electron microscopy (SEM) and Energy-dispersive X-ray spectroscopy(EDX)

Scanning electron microscopy (SEM) is a technique that use electron beam for scanning the sample’s surface point by point, then get the image of the whole surface of the sample.

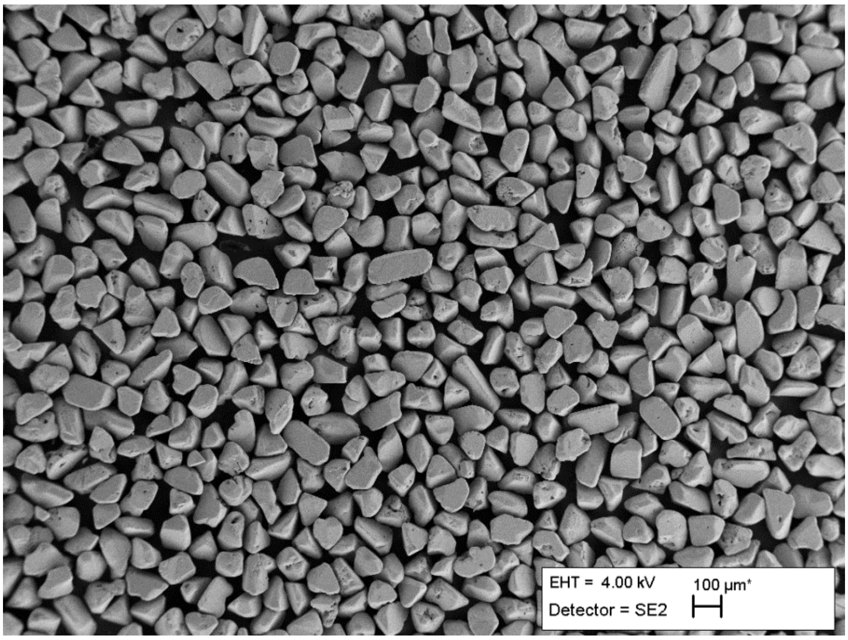

Figure 4. SEM image of CZTSe membrane's surface

Figure 4 shows an example of SEM image from the surface of CZTSe membrane. From this graph we can get some information: about the shape and size of the crystals, are they homogeneous or not and what is the morphology of the crystals surface. Then we can decide are these crystals good or not.

Energy-dispersive X-ray spectroscopy (EDX) is a technique that is used for the elemental analysis or chemical homogeneity characterization of a sample (different compounds could be detected). There is an X-ray source (electron beam or x-ray beam) for the excitation of sample inside the machine, then there is an interaction between the samples and X-ray. The characterization capabilities are relied on the unique atomic structure of each element which allows a unique set of peaks on its electromagnetic emission spectrum [51].

3.1.3. *I-V* curve measurement of solar cell

The main characteristics of solar cell are open circuit voltage V_{oc}, fill factor FF, short circuit current I_{sc} and efficiency η, and they can be derived from *I-V* curve measurements. The main parameters maximum possible delivered energy, $P_{mp}=V_{mp}\cdot I_{mp}$ are shown in figure 5. The main parameter is the power conversion efficiency of solar cell $\eta=V_{oc}\cdot I_{sc}\cdot FF/P_{in}$, where P_{in} is the power density of exiting illumination. In the figure we can see power at the maximum power.

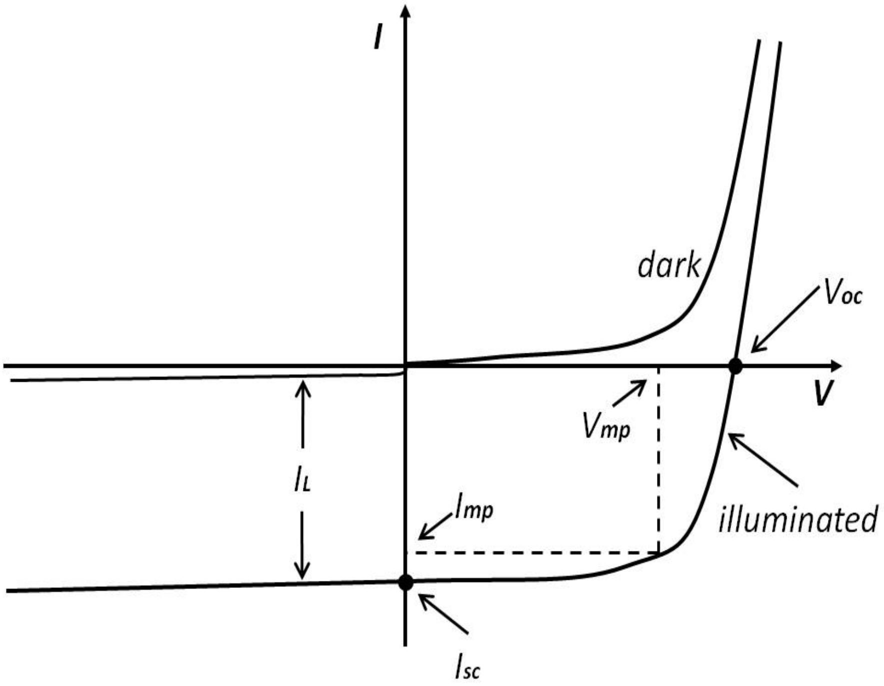

Figure 5: I-V characteristics of a solar cell at non-illuminated (dark) and illuminated conditions [52].

point (*Pmp*) as the maximum square area (power), this power can be calculated by the equation: $Pmp=Vmp\cdot Imp$. The next important parameter is fill factor (*FF*), it shows the ratio of *Pmp* to the product of $Voc\cdot Isc$, and this parameter shows how the square area accounts the whole square area formed from measured V_{oc} *and* I_{sc} then we can know the output characteristic [53].

$FF=V_{mp}\cdot I_{mp}/V_{oc}\cdot I_{sc}$

Usually a perfect solar cell has the fill factor between 0.7-0.85, and the energy–conversion efficiency, η can be written as:

$\eta=Voc\cdot Isc\cdot FF/Pin$ [54].

Pin is the power density of exiting illumination or the power density of solar energy falling to solar cell under illumination conditions. Usually for commercial solar cell, the conversion efficiency is around 12%-14% [54]. In order to make a perfect solar cell, there should be some research work for optimizing the main four parameters of the solar cell: fill factor - *FF*, efficiency - η, open circuit voltage - *Voc* and current density - *Isc*. However, usually when we want to increase one parameter, the others will drop, so the best way is to consider the optimal efficiency of the solar cell [53].

3.2. Experimental procedure

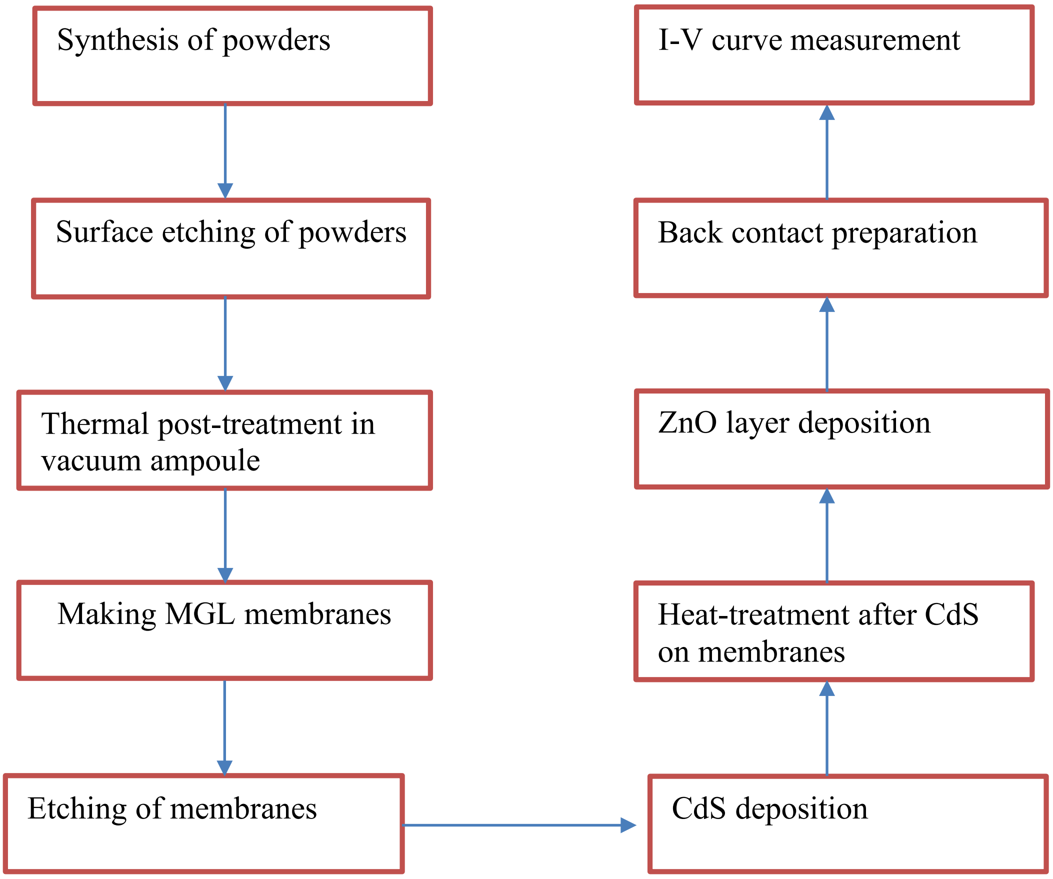

3.2.1. Synthesis of powders

In the thesis the CZTSe monograin powder N221 was used. The powder was synthesized at 700°C in molten KI and grown for 95 hours. Input composition was: $Cu_{1.8}Zn_{1.1}SnSe_{3.9}$+15%Se. Composition after synthesis (as grown) was determined by EDX as $Cu_{1.74}Zn_{1.1}SnSe_{3.85}$. After washing out KI, the powder was sieved into several size fractions. The sieves with different hole sizes (μm) were used for sieving absorber material for making monograin membrane solar cell (before every sieving process, the sieve should be cleaned by compressed air).

3.2.2. Chemical etching of powders and MGL membranes

After sieving process, the powder was etched with 1% Br_2-MeOH solution for 1 minute and KCN (10% KCN+1%KOH) solution for 1.5 minutes. Most importantly, after each step, the membranes should be rinsed with deionized water for 10 times.

For etching MGL membranes, we used different etchants at room temperature for different times and different concentrations, the solution should be under stirring during the etching process.

3.2.3. Thermal annealing of CZTSe-absorber material in Se vapor

The powders were sealed (under vacuum) into a 2-zone quartz ampoule (see Figure 6) and heat-treated at different temperatures in a 2-zone furnace under Se vapor for 1 hour. Elemental Se was also sealed into the same ampoule. Selenium was fixed by melting it onto quartz tube before sealing the ampoule in flame.

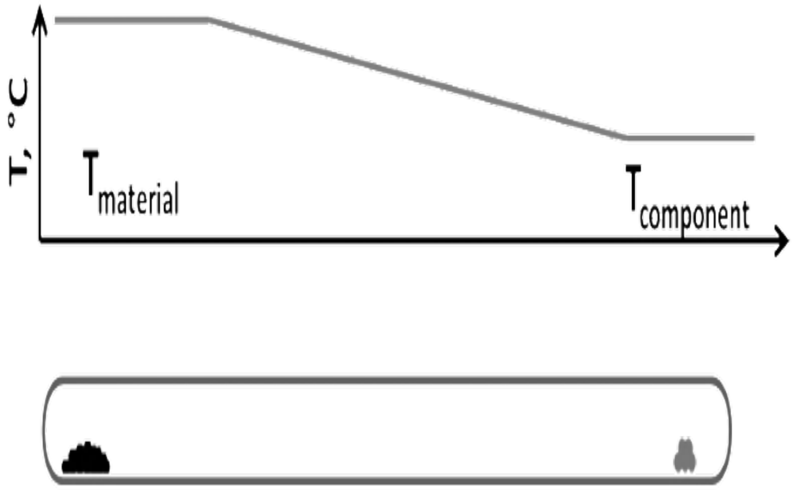

Figure 6. Temperature difference in furnace for heat-treatment of powders in 2-zone arrangement and a quartz ampoule with CZTSe powder in the left end and Se in the right end [55].

3.2.4. Making CZTS MGL membranes

After thermal annealing of CZTSe monograin powder in Se vapor the MGL membranes were made from the powders by our research group member PhD Tiit Varema. He used plastic substrate, epoxy and monograin powders for membrane making, a good membrane should be with thin epoxy and uniform distribution of the grains (see Figure 4).

3.2.5. Chemical solution deposition of buffer layers

The recipe that we used for CdS deposition is given in the Table 1. The ammonia and Cd-ion solutions were mixed together 5 minutes before thiourea was added and the membranes were dipped into solution. Then the deposition solution was heated up to 50°C in a hot water bath. After 20 minutes the CdS deposition was stopped by taking the membranes out of solution. Rinsing of membranes after CdS deposition was made with DI water stream. All the membranes covered with CdS were heated in a thermostat or in quartz tubes at different temperatures.

3.2.5.1. Experimental set-up for CdS deposition onto membranes

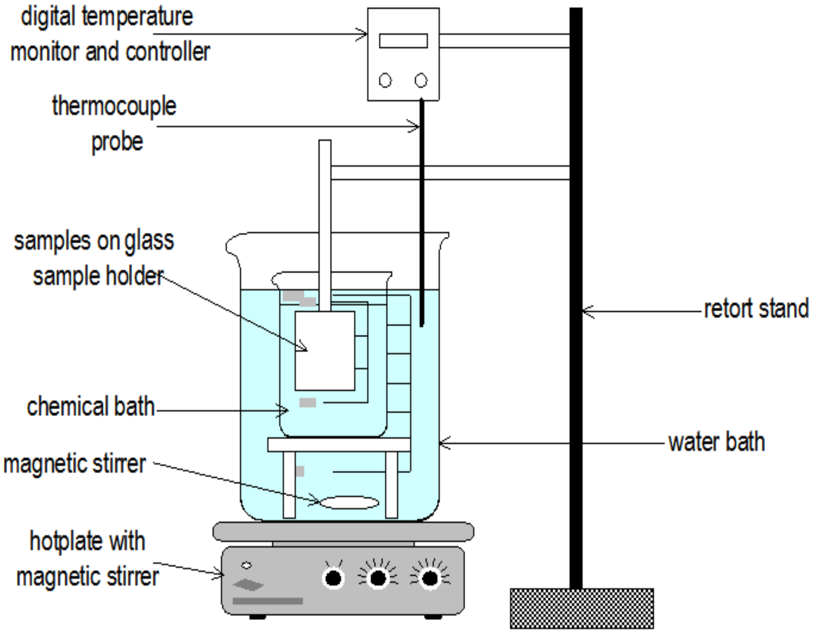

Figure 7. Set-up for chemical bath deposition [56].

The scheme of the chemical bath deposition device is shown in Figure 7: A beaker filled with aqueous solution of precursors for deposition is in a water bath which is placed onto a hot plate equipped with temperature controller and magnetic stirrer which controls the heating and stirring rate. Membranes are fixed into a substrate holder; the reaction bath solution level should be higher than the top of the membrane. Used process is a “cold start” process (continuously heated up from room temperature up to 50°C). Last but not least, as there is ammonia in the bath solution and it is volatile and easily evaporating and has a strong irritating vapor, so the beaker with solution should be covered with a lid to avoid evaporation of ammonia.

3.2.5.2. Experimental procedure for CdS deposition on powders

A reagent bottle (50 ml) with lid was used as a reactor. Powder was put into the bottle, chemical bath solution for CdS was poured also into the bottle and the deposition process similar as described for membranes, was proceeded by shaking the bottles by hands. After deposition process, solution was removed by decantation and powder was rinsed with deionized water for several times.

3.2.6. ZnO layer deposition

i-ZnO and ZnO:Al window layers were deposited by radio-frequency sputtering deposition process, this step was done by our research group members Tiit Varema and Maris Pilvet. Then the membranes were framed by silver paste, covered with silver nanowire ink and a graphite dot for front contact, then the membranes were glued onto glass substrates by epoxy for more safe handling during *I-V* measurement.

3.2.7. Preparation of back contacts of solar cell samples for *I-V* curve measurements

After hardening of epoxy the transparent plastic film substrate used as an initial undercoat for membrane was removed from the back side of the membranes. Now the surfaces of CZTSe crystals from the back side of solar cell membrane were released from epoxy by etching with concentrated sulfuric acid followed by abrasive treatment with sand paper. The etching with H_2SO_4 should be done carefully, the first etching process time is around half minute, then after checking in an optical microscope the membranes should be etched again, until all the crystals are exposed from the surface. After that, the opened crystals should be polished with sandpaper by hand. Graphite ink was used for making dots for contacting back side of MGL solar cell. After determination of area of graphite dots (ordinarily 0.04-0.06 cm^{-2}) the parameters of the solar cell were determined from current-voltage (*I-V*) measurements.

Table 1. The precursor solutions for cadmium sulfide chemical bath deposition and recipe for CdS deposition (process started at room temperature, solution was heated up to 50°C, deposition time=20 minutes, pH=11.4).

Precursor solutions	Concentration of precursor solutions (mole/L)	Volume for 160 ml of deposition solution, mL	Concentration in CBD solution (mole/L)
$Cd(NO_3)_2$	0.01	22.4	0.0014
NH4OH	2	84.0	1.05
$(SC(NH)_2)_2$	1	22.4	0.07
H_2O		31.2	

Table 2. The precursor solutions and recipe for indium sulfide chemical bath deposition (process started at room temperature, solution was heated up to 50°C, deposition time=5 minutes).

Precursor solutions	Concentration, (mole/L)	Volume for 100 mL of deposition solution (mL)	Concentration in CBD solution (mole/L)
In_2Cl_3	2	1.25	0.025
Thioacetamide (TAA)	1	35	0.35
H_2O		63.75	

Table 3. Physical analysis methods

Characterization methods	Properties	Operator
SEM, EDX	Morphology, thickness, grain size, elemental composition	Valdek Mikli
PL	Indication of level of recombination	Taavi Raadik
Raman spectroscopy	Phase composition	Maarja Grossberg
I-*V* measurement	Solar cell characteristics	Kang Zhong

4. RESULTS AND DISCUSSIONS

4.1. Influence of heat-treatment after CdS deposition to the characteristics of CZTSe monograin layer

CdS was deposited by two-fold deposition process onto the as-grown nonetched CZTSe powder crystals. A cross-sectional SEM image of a CdS layer is presented in the Figure 8. The powder covered with CdS was devided into several portions and heated at different temperatures for constant time (for 10 minutes) and at 200°C for different times: 5, 10, 15, 20 and 30 minutes. These differently heated powders were used for making absorber membranes for solar cells

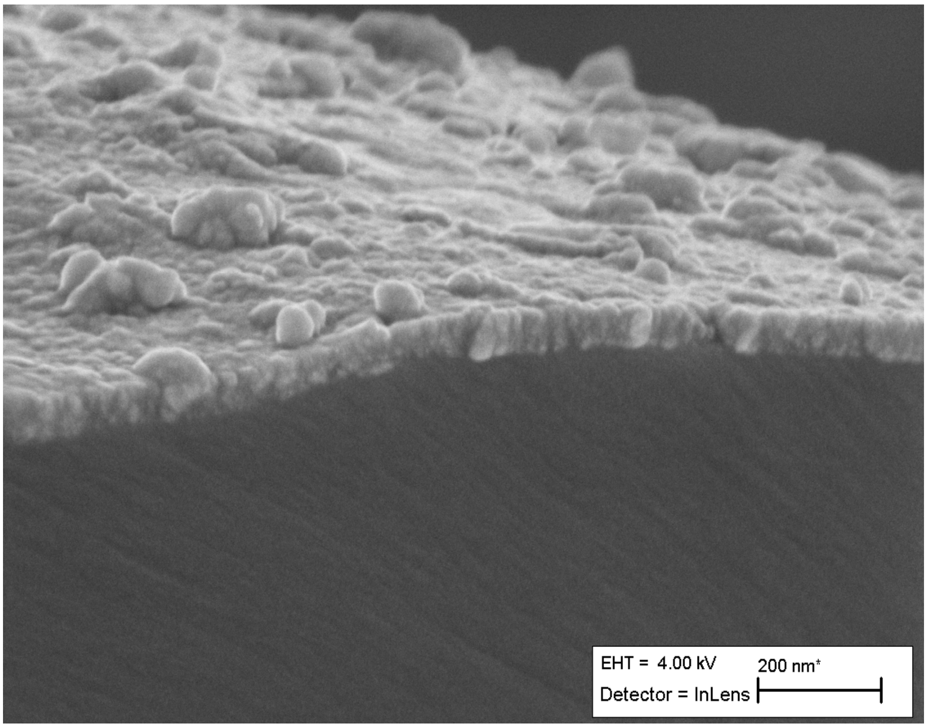

Figure 8. Cross-sectional SEM images of CdS film, deposited for 20 minutes at 50°C, thickness of film is about 50-60 nm

Figure 8 shows the thickness (50-60 nm) and morphology of CdS buffer layer on CZTSe membranes. It could be seen, that the layers are continuous, with good coverage and without pin holes. The number of big colloidal particles on surface is rather high. It can influence to the electrical properties of the whole solar cell structure because colloidal particles can increase the series resistance, so the solar cell will lose some current value.

4.1.1. Influence of heat-treatment temperature after CdS deposition to CZTSe monograin layer solar cell parameters

The parameters of solar cells made from powders heated at different temperatures for constant time (for 10 minutes) after CdS deposition are presented in Figure 9.

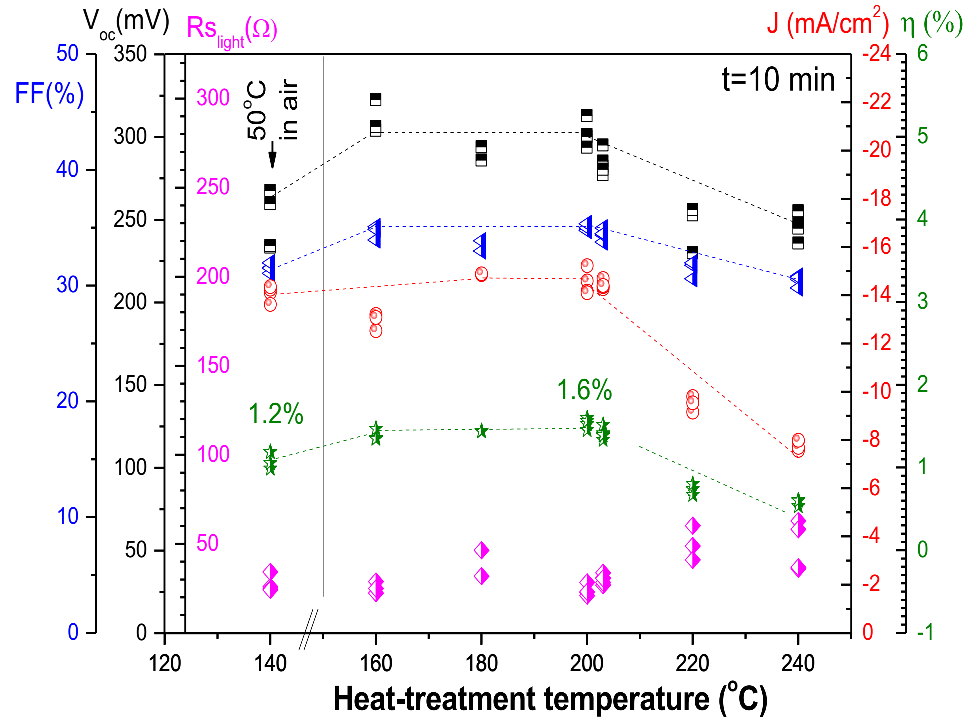

Figure 9. Characteristics of CZTSe MGL solar cells with CdS buffer layers heat-treated at different temperatures for constant heat-treatment time (10minutes).

Figure 9 shows the influence of different heat-treatment temperatures both under continuous vacuum pumping (right side from the vertical line) and in air (left from the vertical line), time is constant (10 minutes) for all the used heating temperatures. The experiment was done with the aim to find out the optimal heat-treatment conditions by changing the temperature from 50°C to 240°C. All the solar cell parameters on the base of powders heated at temperatures higher than 160°C have been increased (current density, fill factor, open circuit voltage, solar cell efficiency) in comparision with heat-treatment in air at 50°C. Heat-treatments at 220°C and 240°C for 10 minutes resulted in solar cells with lower parameters. The highest value of solar cell efficiency was 1.6% when temperature was 200°C. So, the temperature region

160°C to 200°C is the optimal for heat-treatment after CdS deposition for the CZTSe-based solar cells.

4.1.2. Influence of heat-treatment time at constant temperature to CZTSe monograin layer solar cell parameters

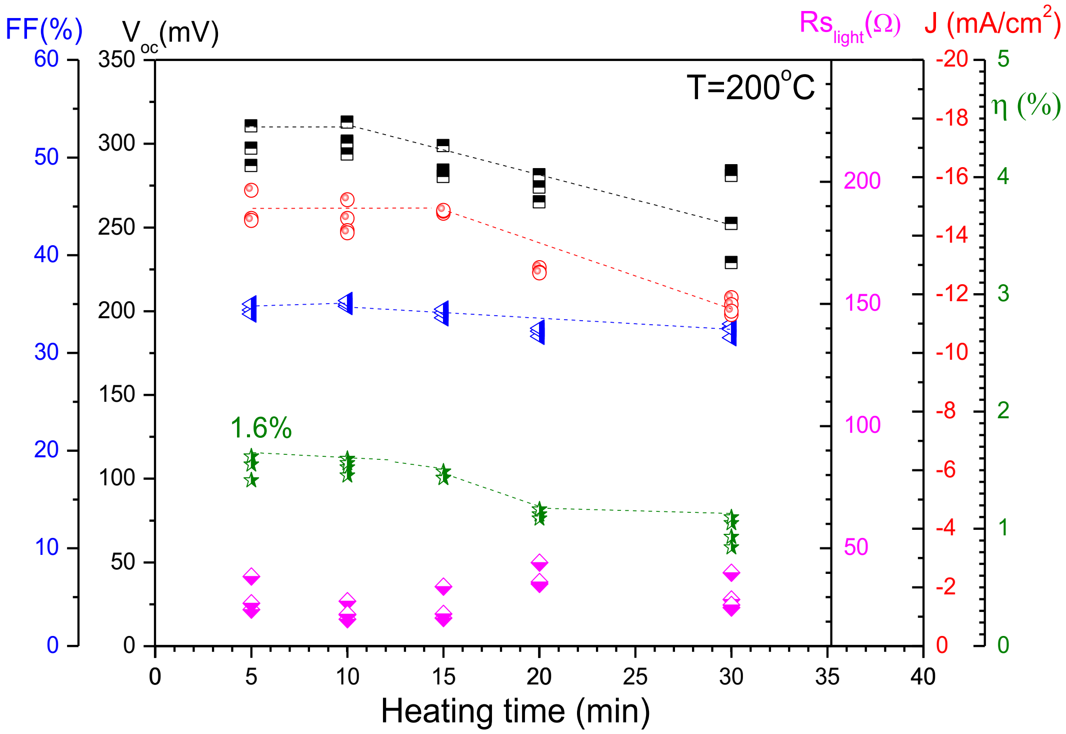

Figure 10. Characteristics of CZTSe MGL solar cells with CdS buffer layers versus heat-treatment time. Heat-treatment temperature 200°C.

Figure 10 shows that by increasing the heating time from 5 to10 minutes, all the parameters of the solar cell stay almost constant, the efficiency is around 1.6%. After 10 minutes of heat-treatment, all the parameters, except fill factor, were decreased, while the fill factor value remains almost constant at around 35%. At the heating time of 30 minutes, the performance of the solar cells dropped to the lowest value in this series. In conclusion, we can say that heat-treatment for 5 to 10 minutes at 200°C is the optimal heat-treatment after CdS deposition for the CZTSe-based solar cells.

4.2. Influence of thermal annealing of CZTSe absorber powder in Se vapor to CZTSe MGL solar cells performance

The CZTSe monograin powder used in this part was etched for 1 minute with 1% bromine solution in methamol followed by etching for 1.5 minutes in KCN solution. Thermal annealing of absorber material was done for 1 hour in 2-zone ampoules, where the CZTSe absorber material was at 650°C and different Se vapor pressure was achieved by different temperatures of the other end of the ampoules.

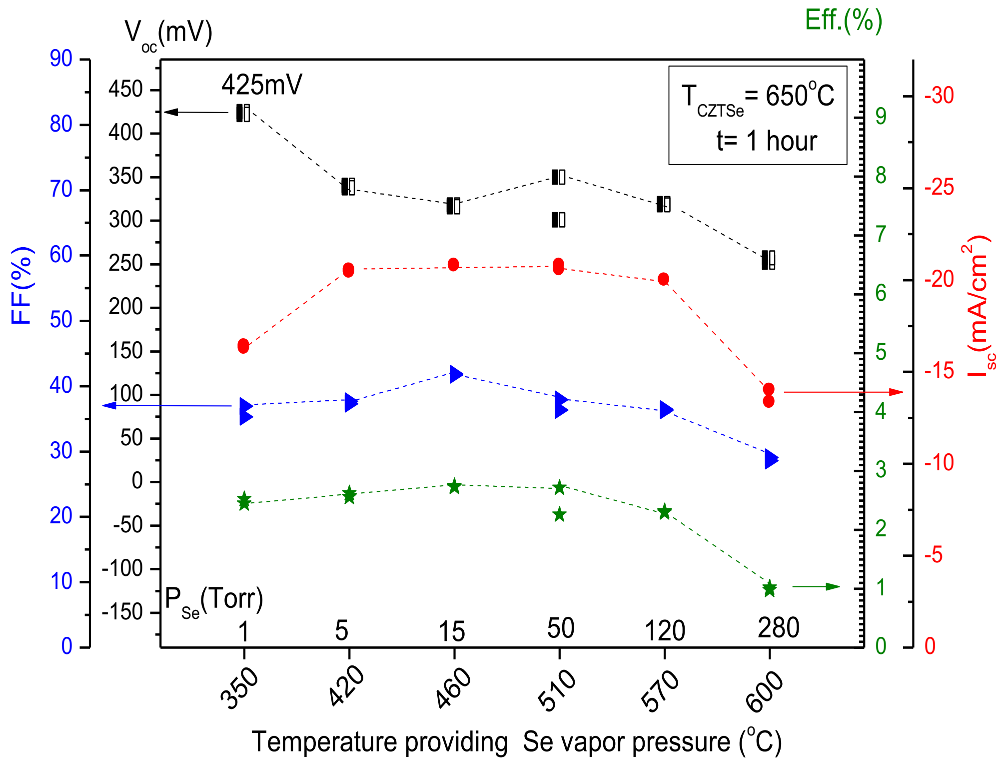

Figure 11. Characteristics of CZTSe monograin membrane solar cells versus applied temperature of Se side in 2-zone ampoules. Thermal annealing of absorber material was done at 650°C in Se vapors for 1 hour. Vapor pressure of Se is determined by applied temperature of Se side. MGL membranes got complex (so called "standard") etching (5 seconds with concentrated HCl and 5 seconds 1% Br_2-MeOH solution and 5 seconds KCN (10% KCN+1%KOH) solution) before CdS deposition and they were heated after CdS deposition at 160°C for 10 minutes in air.

Figure 11 shows the influence of applied Se vapor pressure in thermal annealing to the performance of CZTSe monograin membrane solar cells. The powders were sealed (under vacuum) into 2-zone quartz ampoules with Se in the other end of ampoule and heat-treated at 650°C/350°C, 650°C/420°C, 650°C/460°C, 650°C/510°C, 650°C/570°C, 650°C/600°C for 1 hour (thermal annealing of absorber material was done at 650°C in Se vapors for 1 hour. Vapor pressure of Se is determined by applied temperature of Se side see Figure 6).

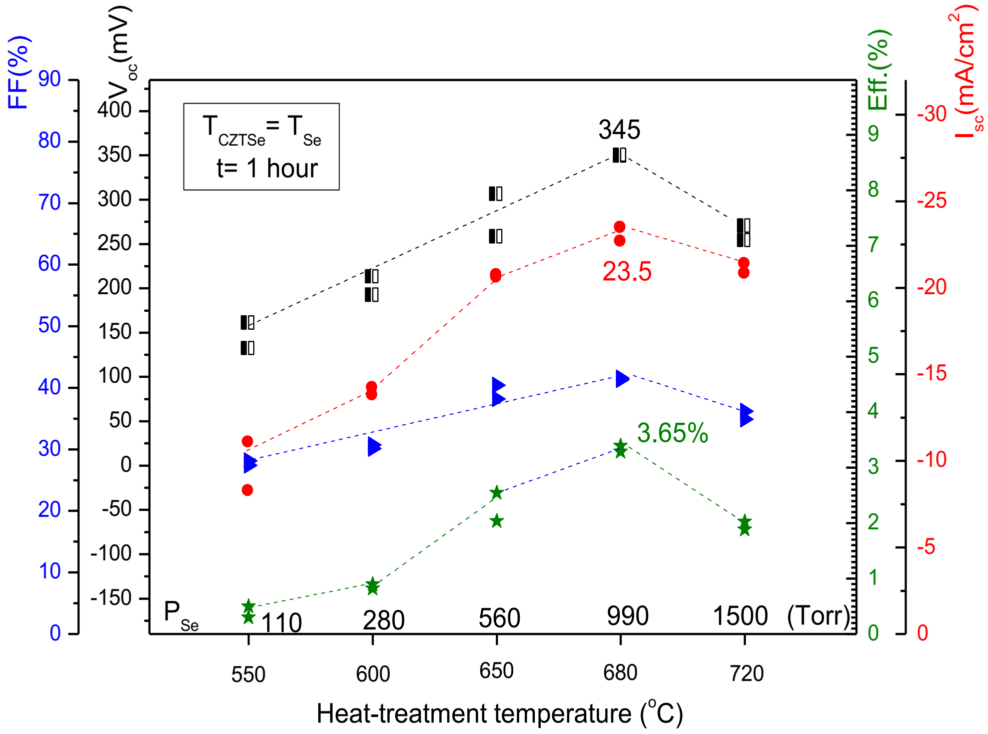

Figure 12. Characteristics of CZTSe monograin membrane solar cells versus applied heat-treatment temperature of CZTSe absorber material in 2-zone ampoules. Heating time 1 hour. Temperatures of material side and Se side were the same. MGL membranes got complex etching (5 seconds with concentrated HCl and 5 seconds 1% Br_2-MeOH solution and 5 seconds KCN (10% KCN+1%KOH) solution) before CdS deposition and they were heated at 160°C for 10 minutes in air after CdS deposition.

At 350°C for Se vapor, the solar cell shows the best open circuit voltage 425mV, while the current density is lower, maybe due to higher resistance, so we have lost some current value. Then with increasing temperature of Se, (Se vapor pressure is increasing), the solar cell parameters remain at almost the same level. When the temperature of Se side is increased up to 600°C, the performance of the solar cells decreases.

Figure 12 shows the influence of thermal annealing of absorber material in 2-zone ampoules at different temperatures while temperatures of the both zones are the same to the performance of CZTSe monograin membrane solar cells. The powder was sealed (under vacuum) into a 2-zone quartz ampoule with Se and heat-treated at 550°C/550°C, 600°C/600°C, 650°C/650°C, 680°C/680°C, 720°C/720°C for 1 hour. (Characteristics of

CZTSe monograin membrane solar cells versus applied temperature of CZTSe absorber material heat-treatment in 2-zone ampoules for 1 hour. Temperatures of material side and Se side were the same). It can be seen that the solar cell performance increases with increasing heat-treatment temperature and at 680°C/680°C annealing conditions shows the best open circuit voltage (345 mV), fill factor, current density (23.5 mA/cm^2) and efficiency (3.65 %) values. So, from these data we can conclude that for this CZTSe absorber material, annealing conditions at 680°C/680°C are the optimal for increasing the performance of the CZTSe MGL solar cell.

4.2.1 Composition of powders thermally heated in Se vapor

The bulk composition of powder crystals heated in Se vapor in different conditions was determined by EDX from polished samples.

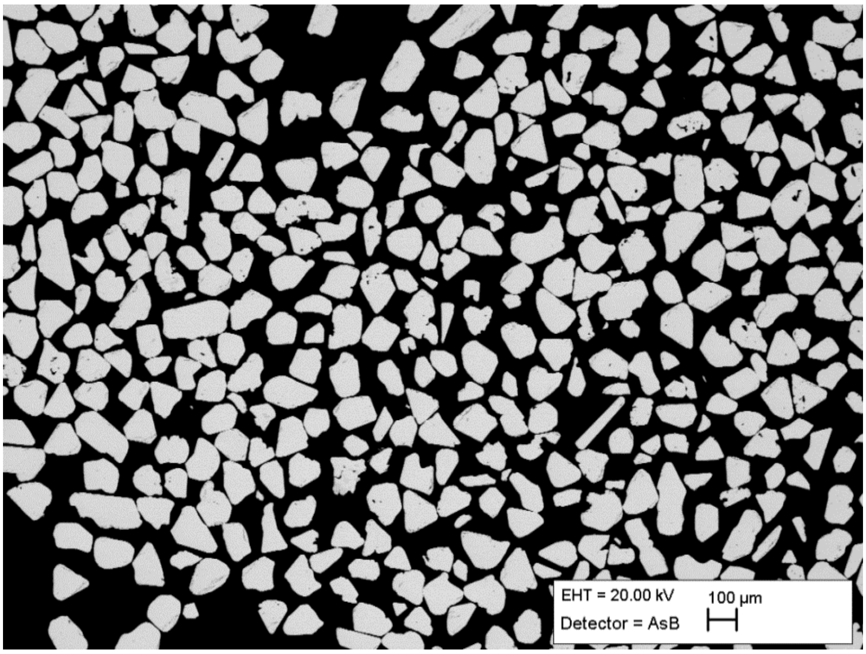

Figure 13. SEM image of a polished sample of monograin powders thermally annealed in Se vapor.

In Figure 13, we can see a SEM image of annealed and polished CZTSe crystals. All the powders annealed under different heat-treatment conditions look similar and uniform, we can’t see big differences in the morphology.

EDX analysis data are presented in Figure 14. The lower part of the Figure 14 presents the concentrations of individual elements and the upper part shows the concentration ratios [Cu]/([Zn]+[Sn]), [Zn]/[Sn] and [Se]/([Cu]+[Zn]+[Sn]), marked as Cu/(Zn+Sn), Zn/Sn and Se/M, respectively.

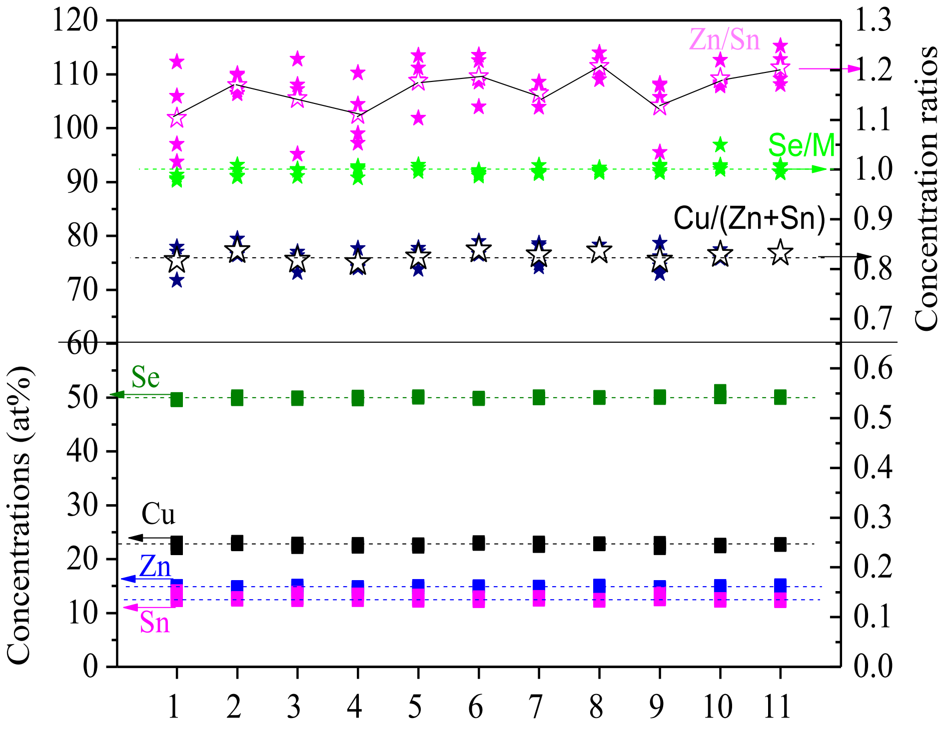

Figure 14. Compositions of differently annealed in Se vapor powders determined by EDX. The x-axis values 1-11 correspond to the different heat-treatments of absorber materials of solar cells in Figures 11 and 12 (temperature of CZTSe powder/temperature of Se):1-650°C/350°C, 2-650°C/420°C, 3-650°C/460°C, 4-650°C/510°C, 5-650°C/570°C, 6-650°C/600°C, 7-550°C/550°C, 8-600°C/600°C, 9-650°C/650°C, 10-680°C/680°C, 11-720°C/720°C. The upper part shows the concentration ratios [Cu]/([Zn]+[Sn]), [Zn]/[Sn] and [Se]/([Cu]+[Zn]+[Sn]), marked as Cu/(Zn+Sn), Zn/Sn and Se/M, respectively.

From the EDX analysis data we can see that these 11 different heat-treatments did not change the elemental composition of powder crystals. It is a hint to the situation that the composition of the absorber material is inside the homogeneity region of the phase diagram of CZTSe.

4.3. Influence of different chemical etching conditions to CZTSe solar cells' performance

The CZTSe absorber material after synthesis at high temperature, this synthesis process will bring some secondary phases onto the crystal's surface, if these phases are stayed at the surface of CZTSe/CdS interface, the open circuit voltage value will decrease, that will decrease the performance of solar cell. The etchants are used for purifying the crystals' surface (remove secondary phases).

4.3.1. Influence of chemical etching to the phase composition of as grown CZTSe powder crystals' surface

Raman spectra of the as grown CZTSe powder are shown in the Figure 15 and the Raman spectra of the chemically etched powder are presented in the Figure 16.

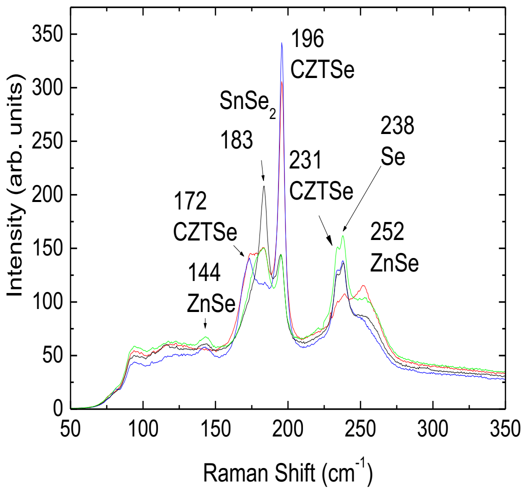

Figure 15. Raman spectra of as grown monograin powder (bulk composition is analyzed by EDX as $Cu_{1.74}Zn_{1.1}SnSe_{3.84}$*).*

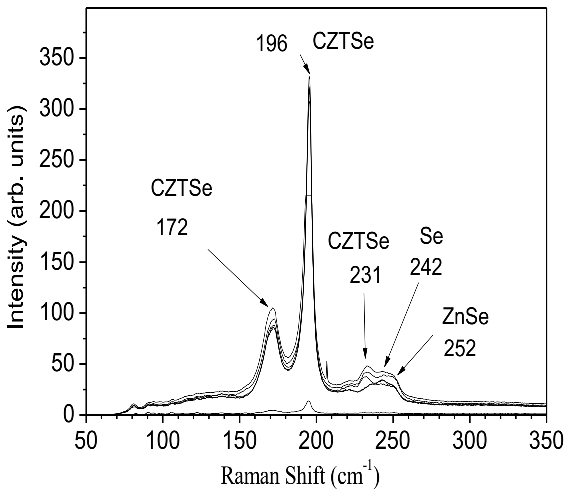

Figure 16. Raman spectra of monograin powder with composition $Cu_{1.74}Zn_{1.1}SnSe_{3.84}$*) etched for 1 minute with 1%* Br_2*-MetOH solution followed by etching for 1.5 minutes in KCN (10% KCN+1%KOH) solution.*

In Figure 15, we can see Raman spectra of the as grown powder. Besides main peaks of CZTSe at 172 cm^{-1}, 196 cm^{-1}, 231 cm^{-1} [57] we can see also the Raman peaks of ZnSe at 144 cm^{-1} and 252 cm^{-1} [58] and the main peak of $SnSe_2$ binary compound at 183 cm^{-1} [59]. Elemental Se can be recognized by its Raman peak at 238 cm^{-1} [60]. We can conclude from Raman spectra that the surface of as grown material is not clean. Raman spectra of monograin powder etched for 1 minute with 1% Br_2-MetOH solution followed by etching for 1.5 minutes in KCN (10% KCN+1%KOH) solution are presented in Figure 16. In addition to the main peaks of CZTSe at 172 cm^{-1} ,196 cm^{-1} and 231 cm^{-1} [57], ZnSe at 252 [58] and Se peak at 242 cm^{-1} [60] is seen. It means that the used chemical etchings have not cleaned thoroughly the surface of the crystals.

4.3.2. Influence of different chemical etching conditions before CdS deposition to the thermally annealed CZTSe powder crystals' surface

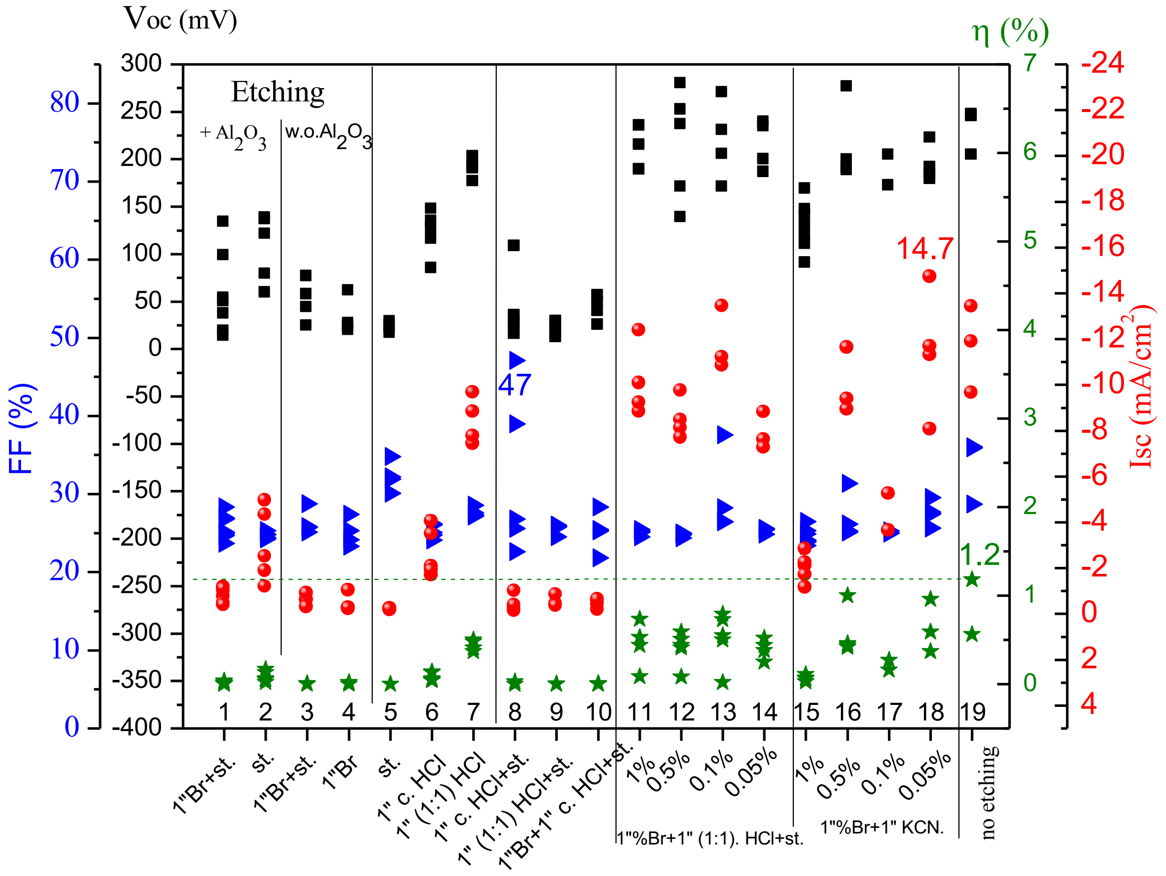

Figure 17. Influence of different chemical etchings to the performance of CZTSe MGL solar cell. The individual membranes for different etchings were cut from the same long MGL membrane. "st." marks so called "standard" complex etching: etching for 5 seconds with concentrated HCl followed by 5 seconds with 1% Br_2-MeOH solution followed with etching for 5 seconds with KCN (10% KCN+1%KOH) solution.

The experiments made in this part were performed using CZTSe powder synthesized and grown at 700°C in molten KI for 95 hours. After that, the powder was etched with 1% bromine solution in methanol for 3 minutes followed by KCN (10%KCN+1%KOH) etching for 4.5 minutes. Then the powder was heated in isothermal conditions at 680°C in Se vapor for 1 hour followed by fast cooling.

The CZTSe/CdS solar cells characteristics are shown in the Figure 17. Changing of the etching conditions before CdS deposition, shown in the Figure 17 at x-axes positions, did not improve the solar cell performance in comparison with the solar cell performance that was not etched before CdS deposition (position 19 in the Figure 17). The best solar cell efficiency 1.2% was got from solar cell on the base of absorber without chemical etching before CdS deposition. All the other solar cells showed lower conversion efficiency. It means that chemical etchings can decrease or increase solar cell properties easily, but not to improve materials bulk properties, that are mainly determining the final solar cell energy conversion ability. 1.2% efficiency measured for the best solar cell in this series is very low indicating that the used CZTSe material (etched and heat-treated) was not with the best properties. Some trends could be seen: comparing solar cell performances of etched with concentrated HCl and with diluted HCl (H_2O: HCl=1:1), it is obvious that the open circuit voltage and current density and efficiency values are higher if diluted HCl etching was used (compare positions 6 and 7 in the Figure 17). By adding Al_2O_3 intermidiate layer, only the voltage value increased a little, other parameters remains almost the same level. From Raman spectra (see Figure 16) we know that some ZnSe have been remained onto CZTSe crystals' surface, therefore we can consider, that etching with diluted HCl removes ZnSe better than etching with concentrated HCl. The following "standard" etching had lowered solar cell performance, compare the data at 7 with those at 8 and 9 in Figure 17.

It is known from previous experimental work with CZTSSe absorber materials, that photoluminescence (PL) intensity of absorber material can serve as indicator of recombination level on *p-n* junction, it means that the brighter is PL intensity, the more effectively p-n junction can work. We measured PL intensity of CZTSe absorber material after different chemical etchings. The PL spectra of these materials are presented in the Figure 18 and in the Table 4. It is seen that the PL spectra have the same shape but different intensities. The lowest PL intensity has the material, etched for 10 seconds with concentrated HCl, while the etching for 30 seconds increases the PL intensity more than 18 times (from 81 to 1504, see Table 4).

The reference powder and the powders etched with KCN have similar PL intensities (2400-2500 arb.u.). The powder etched by the “standard” etching process (for 5 seconds with concentrated HCl followed by 5 seconds with 1% Br_2-MeOH and finally for 5 seconds with KCN (10%KCN+1%KOH) solution show the highest PL intensity. We can see that the crystals’ surface is so sensitive to etchings, even if the same etchant is used for etching, longer or shorter time will have different influence. The reference powder shows the intensity of 2531 arbitrary units, which is lower than the best result. Thus the so called “standard” etching (5 seconds concentrated HCl + 5 seconds 1% Br_2-MeOH + 5 seconds KCN (10%KCN+1%KOH) solution) is the best good for decreasing the recombination level, hence increasing the performance of the CZTSe-based solar cell if the material is heat treated by the best way.

a)

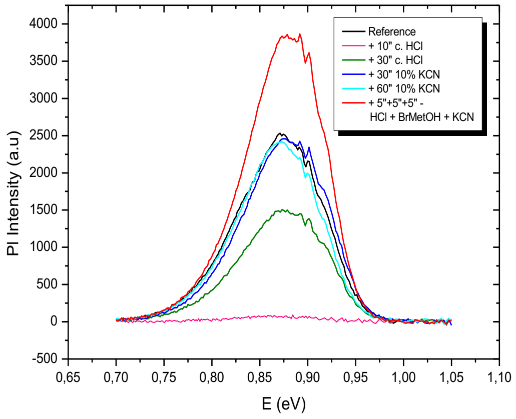

b)

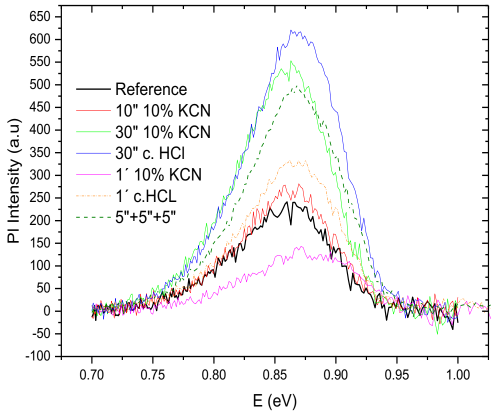

Figure 18-a: Photoluminescence spectra (at 10K) of differently etched CZTSe monograin powders. Reference – as-grown powder, etched for 3 minutes with 1% Br_2-MeOH solution followed by 4.5 minutes with KCN (10% KCN+1%KOH) solution.

Figure 18-b: Photoluminescence spectra (at 10K) of differently etched CZTSe monograin powders with thermal annealing at 680°C/680°C in Se vapor. *Reference – as-grown powder, etched for 3 minutes with 1% Br_2-MeOH solution followed by 4.5 minutes with KCN (10% KCN+1%KOH) solution.*

Figure 18 (a and b) show different photoluminescence spectra of different etching conditions, we can see the etching condition from Figure 18-a (5 seconds concentrated HCl + 5 seconds 1% Br_2-MeOH + 5 seconds (KCN (10%)+ KOH (1%)) solution) can increase the intensity value then decrease the recombination of the electrons and holes. However, some etching conditions (10 sec. HCl) can also increase the the recombination rate, hence decrease the performance of the solar cell.

Figure18-b shows after thermal annealing at 680°C/680°C, the intensity value for all etching conditions are decreased, that means the thermal annealing condition is not good for decreasing the recombination rate of the solar cell.

4.4. Influence of different intermediate layers

4.4.1. Influence of In_2S_3 intermediate layer

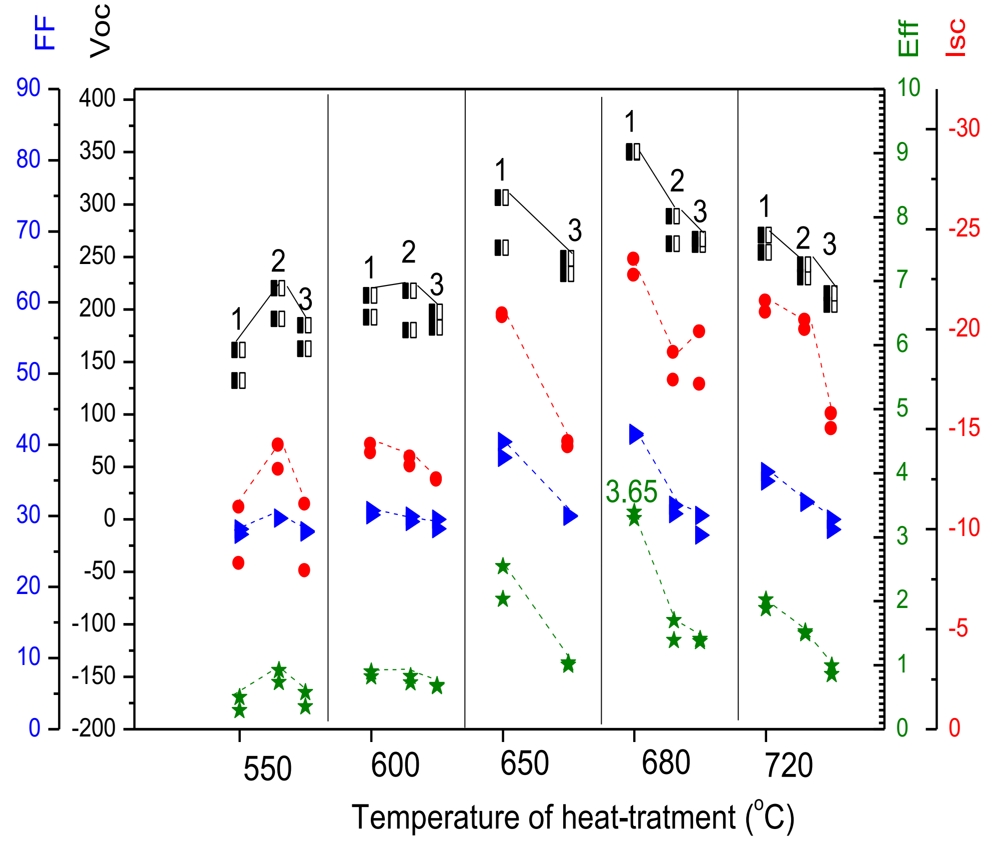

Figure 24. Influence of different intermediate treatments to the performance of CZTSe monograin membrane solar cells made from powders heat-treated at different temperatures in ampoules with Se source at the same temperature. 1- solar cell characteristics as shown in the Figure 12 ("standard" complex etching was done before CdS deposition and heat-treatment at 160°C for 10 minutes in air after CdS deposition); 2-CdS was removed by concentrated HCl and CdS buffer layer was deposited again followed by heating at 160°C for 10 minutes in air; 3- In_2S_3 was deposited onto CdS, heated at 160°C for 10 minutes in air, removed by etching with concentrated HCl and CdS was deposited again followed by heat-treatment at 160°C for 10 min in air.

In this part the influence of possible doping of absorber layer surface due to inter-diffusion of elements from buffer material to absorber material and vice versa was studied. CdS was deposited on the MGL membranes made from the heat-treated powders presented in the part 4.2 (Figure 12). The membranes used in the part 4.2 and here in 4.4 are parallel samples cut from the same membrane. The solar cell characteristics determined by *I-V* measurements are presented in the Figure 24.

From Figure 24, we can see that there are nearly no changes in solar cell characteristics due to multiple etchings, heat-treatments and another deposition processes if the absorber materials were primarily heat-treated under 550°C/550°C and 600°C/600°C annealing conditions. Solar cells made from absorber materials annealed at higher temperatures were much more sensitive to intermediate etchings, depositions and heat-treatments and their characteristics decreased remarkably compared with these based on materials of lower temperature treatment. The material from the 680°C/680°C annealing regime resulted in the highest solar cell performance η=3.65%. Unfortunately, we cannot recognize any positive effect of doping from intermediate layers. It is possible that intermediate etchings with concentrated HCl acid were done under uncontrolled way and as it is obvious from PL measurements (see Table 4) etching time has a big impact to the PL intensity.

4.4.2. Influence of Al_2O_3 intermediate layer

We used two methods to deposit Al_2O_3 intermediate layer between the CZTSe absorber and CdS buffer layers - and pulsed laser deposition (PLD). In my thesis, in Figure 25, Al_2O_3 intermediate layer was deposited by ALD method in University of Tartu by Dr. Aivar Tarre, in Figure 17, Al_2O_3 intermediate layer was done by Dr. Sergei Bereznev with PLD method in Tallin University of Technology.

Short description of ALD and PLD methods:
ALD: The principle of this method is based on sequential pulsing of chemical precursor vapors. It used to generate uniform thickness layer without pin holes [62].
PLD: Pulsed laser deposition is a physical vapor deposition technique, where a high-power pulsed laser beam is focused inside a vacuum chamber to strike a target of the material that is to be deposited [63].

Deposition parameters:

For ALD: Deposition device : Atomic layer deposition systems - $Al(CH_3)_3$+H_2O: 60 cycles, at temperature of 100° C in N_2 (chamber pressure 1.8-2.4 MBar).

For PLD: Deposition device : NEOCERA PIONEER 120, conditions: T=160°C; 7 Hz; 200mJ; high vacuum 10^{-5} Torr, 400 pulses.

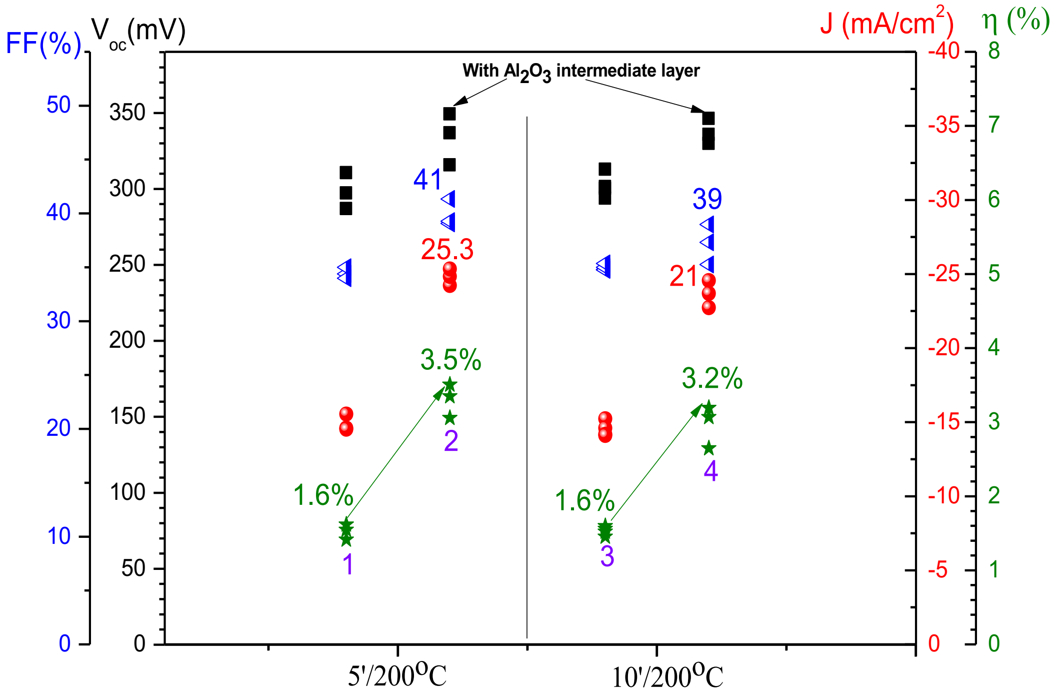

Figure 25. Characteristics of CZTSe MGL solar cells with and without ALD Al_2O_3 intermediate layer. CdS was deposited by two-fold deposition process onto CZTSe powder etched before by "standard" complex etching regime. The powder covered by CdS was heated at 200 °C for 5 minutes (the left side of the Figure25) and for 10 minutes (the right side of the Figure25) before Al_2O_3 deposition. Atomic layer deposition: $Al(CH_3)_3$+H_2O; 60 cycles, at 100° C in N_2 (chamber pressure 1.8-2.4 MBar).

Figure 25 shows the characteristics of MGL solar cells made from membranes with and without Al_2O_3 intermediate layer. Sample number 1(and 3) means that CdS was deposited onto powder 2 times for 15 minutes, then heat-treated in vacuum at 200°C for 5 (or 10) minutes. Sample number 2 (or 4) is a parallel sample to the sample number 1 (or 3), but covered with Al_2O_3 intermediate layer. CdS was removed from surface by HCl before Al_2O_3 deposition and deposited again after Al_2O_3 coverage (samples nr 2 and 4) .We can see from Figure 25, that all the solar cell parameters are sharply increased due to the change in the treatment conditions: compare solar cell characteristics of sample number 1 (3) with these of sample number 2 (4). However, there are several pre-treatment steps changed, not only covered with Al_2O_3: i) HCl etching before Al_2O_3 deposition was done with the aim to remove primarily deposited CdS; ii) an additional heat-treatment in comparison with the sample number 1 because Al_2O_3 deposition process (ALD) itself was done at 100°C for 1 hour in a carrier gas flow. So we could not decide what step is the real reason for this increase in solar cell parameters. Additional studies are needed to do with the aim to find out the real reason of the increase in solar cell parameters.

CONCLUSIONS

The aim of this thesis was to study the possibilities to improve the CZTSe-based solar cells performance by modifying *p-n* junction differently: 1) changing annealing conditions of the CZTSe absorber material in 2-zone ampoules by using different Se vapor pressures and different temperatures; 2) etching absorber material surface chemically with different etchants after heat-treatment; 3) by heat-treatments after CdS deposition by modification of heat-treatment temperature and heat-treatment time in different ambient conditions (closed vacuum, continuous vacuum pumping, air) for improvement the performance of CZTSe solar cells; 4) applying intermediate layers (In_2S_3, Al_2O_3) with the aim to find out some good influence to the performance of CZTSe-based solar cells.

It was found that:

1. The temperature region 160°C to 200°C is the optimal for heat-treatments after CdS deposition for the CZTSe-based solar cells. 5 to 10 minutes is the optimal heat-treatment time after CdS deposition for improving the performance of CZTSe-based solar cell.
2. Heat-treatment of absorber material at 680°C in Se vapor was the most efficient thermal annealing conditions for improving the performance of CZTSe-based solar cells.
3. All the etching conditions we used were not good for improving the solar cell performance, as the CZTSe material is so sensitive to the etchants. However, we can get by using diluted HCl for etching the crystals' surface is better than using concentrated HCl to improve the performance of CZTSe-based solar cell.
4. In_2S_3 intermediate layer in the used testing arrangement did not show any improvement of the working ability of CZTSe monograin layer solar cells.
5. Application of Al_2O_3 intermediate layer into CZTSe monograin layer solar cell improved solar cell efficiency from 1.6 % to 3.5 %. However, in the Al_2O_3 deposition process several pre-treatment steps were changed, and it is difficult to determine which of them had the biggest contribution to the increase of solar cell parameters: Al_2O_3 layer itself or additional HCl etching or additional prolonged heat-treatment at 100°C for 1 hour in a carrier gas flow necessary for Al_2O_3 deposition. Additional studies are needed.

ABSTRACT

One important issue limiting the performance of $Cu_2ZnSnSe_4$ (CZTSe) monograin layer (MGL) solar cells is the circumstance that the crystals' surface is not clean after powder growth, it is covered with different secondary phases dissolved in and precipitated out from the molten phase of the used flux salt in the cooling down period of growth process.The surface coverage could consists of some secondary phases, such as ZnSe, SnSe, $SnSe_2$ or some low bandgap ternary Cu-Sn-Se phases with the Eg below 1eV. If these phases are stayed at the surface of CZTSe or at CZTSe/CdS interface, the open circuit value will decrease, also the whole performance of the solar cell will decrease. Ordinarily these phases are removed by complex chemical etchings and the surface damage of crystals is healed by post-growth heat-treatments. This step can produce another minor surface coverage decreasing solar cell performance.

Originated from the above given circumstances the aim of the present research work was to find out the possibilities to improve the CZTSe-based solar cells performance by modifying *p-n* junction differently: 1) changing annealing conditions of the CZTSe absorber material in 2-zone ampoules by using different Se vapor pressures and different temperatures; 2) etching absorber material surface chemically with different etchants after heat-treatment; 3) by heat-treatments after CdS deposition - modifying heat-treatment temperature and heat-treatment time in different ambient conditions (closed vacuum, continuous vacuum pumping, air); 4) applying intermediate layers (In_2S_3, Al_2O_3) with the aim to find out some good influence to the performance of CZTSe-based solar cells.

In the present thesis previously produced CZTSe monograin powder as MGL solar cell absorber material was used for the planned treatments and for making MGL membranes. The effects of chemical etchings were studied by Raman spectroscopy, by photoluminescence intensity measurements and by solar cell characteristics drawn from current-voltage measurements of MGL solar cells.

It was found that heat-treatment of absorber material at 680°C in Se vapor was the most efficient thermal annealing resulting in the 3.65% of CZTSe MGL solar cell efficiency. The temperature region 160°C to 200°C was found to be the optimal for 5 to 10 minutes heat-treatments after CdS deposition. In_2S_3 intermediate layer in the used testing arrangement did not show any improvement of the working ability of CZTSe monograin layer solar cells. Applying of Al_2O_3 intermediate layer into CZTSe monograin layer solar cell improved solar cell efficiency from 1.6 % to 3.5 %. However, in the Al_2O_3 deposition process several pre-

treatment steps were changed, and it was difficult to determine which of them had the biggest contribution to the increase of solar cell parameters: was it Al_2O_3 layer itself or additional HCl etching or additional prolonged heat-treatment at 100°C for 1 hour in a carrier gas flow necessary for Al_2O_3 deposition. Additional studies are needed.

KOKKUVÕTE

Antud magistritöö on suunatud $Cu_2ZnSnSe_4$ (CZTSe) monoterakihiliste (MTK) päikesepatarede *p-n* ülemineku modifitseerimisele. MTK päikesepataredes töötava absorberkihi saamiseks vajaliku monoterapulbri sünteeskasvatus toimub 700°C juures sulandajana kasutatava soola (KI) vedelfaasis, milles lahustuvad vähesel määral ka sünteesiks vajalikud lähteühendid. Sünteeskasvatuse lõppedes sadenevad need allajahutamisel sulast faasist kristallide pinnale. Seetõttu vajab sünteesitud pulbrite kristallide pind puhastamist keemilise söövituse teel. Keemilisele söövitusele järgnev järelkuumutus taastab söövitustega rikutud pinna, kuid võib siiski jätta mittesoovitud pinnakoostise. Selle pinna modifitseerimiseks kasutatakse antud töös erinevaid lühiaegseid söövitusi, mille mõju väljaselgitamine päikespatarei tööle on üheks töö eesmärgiks. Teiseks uuritavaks alateemaks on pulbri järelkuumutus Se rõhus erinevatel temperatuuridel ja Se aururõhkudel kahetsoonilises katsekorralduses. Esimene ja teine eesmärk on teineteisega tihedalt seotud: kui järelkuumutuse korraldus tagab *p-n* üleminekuks sobiva pinna, siis teistkordne söövitus enne CdS sadestamist polegi vajalik.

Parema kontakti saavutamiseks *p-tüüpi* CZTSe absorber ja *n-tüüpi* CdS puhverkihi vahel uuritakse töös CdS sadestamise järgset kuumutamist erinevatel temperatuuridel ja aegadel.

p-n ülemineku alal toimuvate rekombinatsioonikadude vähendamiseks on kirjanduses pakutud välja õhukese Al_2O_3 kihi (~10 nm) sadestamist enne CdS. Antud töös kasutatakse ka seda võimalust ülemineku modifitseerimiseks.

Töös kasutatakse eelnevalt kasvatatud CZTSe monoterapulbrit, mis jagatakse 13 portsjoniks. Ühte osa söövitatakse kompleksprotsessis (5 sec. konts. HCl + 5 sec. Br-metanoolis + 5 sec KCN) ja kasutatakse CdS sadestamise järgse kuumutamise mõju uurimiseks päikesepatarei omadustele. Teisi pulbriportsjoneid kasutatakse pärast söövitamist (1 minut 1% broomi lahuses, millele järgnes 1,5 minutiline söövitus 10% KCN lahuses) kuumutuskatsete läbiviimiseks kahetsoonilistes ampullides erinevatel Se aururõhkudel. Söövituskatsete mõju pinnakoostisele uuriti Raman-spektroskoopia abil ja iseloomustati fotoluminestsentsi intensiivsuse mõõtmise abil. Erinevate töötluste mõju päikesepatarei tööle hinnati volt-amper mõõtmiste teel.

Leiti et kõige efektiivsemaks osutus termotöötlus 680 °C juures Se aurudes, mille tulemusena saadi 3,65 %-lise kasuteguriga töötav CZTSe MTK päikesepatarei.

Temperatuurivahemik 160-200 ^{o}C oli optimaalne CdS sadestamise järgse 5-10 minutilise kuumutamise jaoks, mille tulemusena suurenes päikesepatarei kasutegur 1,2%-lt 1,6 %-ni.
Leiti, et In_2S_3 vahekihil mõju ei avaldunud antud katsekorralduse puhul.
Al_2O_3 õhukese kihi sadestamine absorberile enne CdS sadestamist suurendas CZTSe MTK päikesepatarei kasutegurit 1,6 %-lt 3,5 % -ni. Analüüsides katsekorraldusi Al_2O_3 sadestamisel ja ilma selleta leiti, et nimetatud parameetrite paranemine võib tuleneda ka Al_2O_3 sadestamisega kaasnevast pikaajalisest kuumutamisest 100 ^{o}C juures Al_2O_3 lähteainete kandegaasi voos. Konkreetsete mõjutegurite väljaselgitamine nõuab edasisi katsetusi.

REFERENCES

[1] W. Wang, M.T. Winkler, O. Gunawan, T. Gokmen, T. K. Todorov, Y. Zhu, and D.B.Mitzi, Adv. Energy Mater. 4,1301465(2014).

[2] P. Jackson, D. Hariskos, R. Wuerz, O. Kiowski, A. Bauer., T.M. Friedlmeier, and M. Powalla, Phys. Status Solidi(RRL)9,28-31(2015)

[3] Fairbrother A, García-Hemme E, Izquierdo-Roca V, et al. Development of a selective chemical etch to improve the conversion efficiency of Zn-rich Cu2ZnSnS4 solar cells[J]. Journal of the American Chemical Society, 2012, 134(19): 8018-8021.

[4] López Marino S, Sánchez Y, Placidi M, et al. ZnSe Etching of Zn-Rich Cu2ZnSnSe4: An Oxidation Route for Improved Solar Cell Efficiency[J]. Chemistry–A European Journal, 2013, 19(44): 14814-14822.

[5] M. Altosaar, J. Raudoja, K. Timmo, M. Danilson, M.Grossberg, J. Krustok, E. Mellikov. Cu$_2$ Zn$_{1-x}$Cd$_x$Sn(SeI-y S)$_4$ solid solutions as absorber material for solar cell. Physica Status Solidi,205(2008), 167-170.

[6] H. Katagiri, K. Jimbo, in Photovoltaic Specialists Conference (PVSC) 37th IEEE, pp. 03516-003521,2011.

[7] J.J Scragg, P.J. Dale, D. Colombara, L.M. Peter, ChemPhysChem 2013, 13, 3035-3046

[8] Renewable Energy Policy Network for the 21st century (REN21), Renewables 2010 Global Status Report, Paris, 2010, pp. 1–80.

[9] Tam Hunt (9 March 2015). "The Solar Singularity Is Nigh". Greentech Media. Retrieved 29 April 2015.

[10] Chu J. Development of Photovoltaic Solar Cell Technology[J]. AAPPS Bulletin, 2012, 22(4).

[11] Aldous S. How solar cells work[J]. How Stuff Works. April 1st, 2000.

[12] http://gunam.metu.edu.tr/old/index.php/solar-technology/pv-working-principles.

[13] Knier G. How do photovoltaics work[J]. Science@ NASA, 2002.

[14] Mellikov E, Meissner D, Varema T, et al. Monograin materials for solar cells[J]. Solar Energy Materials and Solar Cells, 2009, 93(1): 65-68.

[15] Altosaar M, Jagomägi A, Kauk M, et al. Monograin layer solar cells[J]. Thin Solid Films, 2003, 431: 466-469.

[16] Mellikov E, Meissner D, Varema T, et al. Monograin materials for solar cells[J]. Solar Energy Materials and Solar Cells, 2009, 93(1): 65-68.

[17] Bag S, Gunawan O, Gokmen T, et al. Low band gap liquid-processed CZTSe solar cell with 10.1% efficiency[J]. Energy & Environmental Science, 2012, 5(5): 7060-7065.

[18] S. Chen, A. Walsh, J. H. Yang, X. G. Gong, L. Sun, P. X. Yang, J. H. Chu and S. H. Wei, Phys. Rev. B: Condens. Matter Mater. Phys., 2011, 83, 125201

[19] Jeon J O, Lee K D, Seul Oh L, et al. Highly efficient copper–zinc–tin–selenide (CZTSe) solar cells by electrodeposition[J]. ChemSusChem, 2014, 7(4): 1073-1077.

[20] Y.Y. Ma, R.H. Bube J. Electrochem. Soc., 124 (1977), p. 1430

[21] Neuschitzer M, Sanchez Y, López-Marino S, et al. Optimization of CdS buffer layer for high-performance $Cu_2ZnSnSe_4$ solar cells and the effects of light soaking: elimination of crossover and red kink[J]. Progress in Photovoltaics: Research and Applications, 2015, 23(11): 1660-1667.

[22] Nakada T, Mizutani M, Hagiwara Y, et al. High-efficiency Cu (In,Ga) Se_2 thin-film solar cells with a CBD-ZnS buffer layer[J]. Solar energy materials and solar cells, 2001, 67(1): 255-260.

[23] Roy P, Srivastava S K. A new approach towards the growth of cadmium sulphide thin film by CBD method and its characterization[J]. Materials chemistry and physics, 2006, 95(2): 235-241.

[24] M.A. Mughal, M.J. Newell, R. Engelken, J. Vangilder, S. Thapa, K. Wood, B.R. Carroll, J.B. Johnson

[25] M.F. Cansizoglu, R. Engelken, H.-W. Seo, T. Karabacak

[26] M.A. Mughal, M.J. Newell, R. Engelken, J. Vangilder, S. Thapa, K. Wood, B.R. Carroll, J.B. Johnson

[27] Mughal M A, Engelken R, Sharma R. Progress in indium (III) sulfide (In_2S_3) buffer layer deposition techniques for CIS, CIGS, and CdTe-based thin film solar cells[J]. Solar Energy, 2015, 120: 131-146.

[28] Vermang B, Fjällström V, Pettersson J, et al. Development of rear surface passivated Cu (In, Ga) Se 2 thin film solar cells with nano-sized local rear point contacts[J]. Solar Energy Materials and Solar Cells, 2013, 117: 505-511.

[29] Hsu W W, Chen J Y, Cheng T H, et al. Surface passivation of Cu(In,Ga) Se_2 using atomic layer deposited Al_2O_3[J]. Applied Physics Letters, 2012, 100(2): 023508.

[30] M. Altosaar, J. Raudoja, K. Timmo, M. Danilson, M. Grossberg, M. Krunks, T. Varema, E. Mellikov, “Cu2ZnSnSe4 Monograin Powders for Solar Cell Application”, Proceedings of the 2006 IEEE WCPEC-4, 2006, pp. 468-470.

[31] Xie H, Sánchez Y, López-Marino S, et al. Impact of Sn (S, Se) secondary phases in $Cu_2ZnSn(S, Se)_4$ solar cells: a chemical route for their selective removal and absorber surface passivation[J]. ACS applied materials & interfaces, 2014, 6(15): 12744-12751.

[32] Timmo K, Altosaar M, Raudoja J, et al. Chemical etching of $Cu_2ZnSn(S,Se)_4$ monograin powder[C]//Photovoltaic Specialists Conference (PVSC), 2010 35th IEEE. IEEE, 2010: 001982-001985

[33] K.Timmo, M.Altosaar, J.Raudoja, M.Grossberg, M.Danilson, O.Volobujeva, E.Mellikov Department of Materials Science, Tallinn University of Technology, Tallinn, Estonia

[34] Kauk-Kuusik M, Timmo K, Danilson M, et al. p–n junction improvements of $Cu_2 ZnSnS_4$/CdS monograin layer solar cells [J]. Applied Surface Science, 2015, 357: 795-798.

[35] Neuschitzer M, Sanchez Y, Olar T, et al. Complex surface chemistry of kesterites: Cu/Zn reordering after low temperature postdeposition annealing and its role in high performance devices[J]. Chemistry of Materials, 2015, 27(15): 5279-5287.

[36] Mousel M, Redinger A, Djemour R, et al. HCl and Br_2-MeOH etching of $Cu_2 ZnSnSe_4$ polycrystalline absorbers[J]. Thin Solid Films, 2013, 535: 83-87.

[37] Buffiere M, Brammertz G, Sahayaraj S, et al. KCN chemical etch for interface engineering in Cu2ZnSnSe4 solar cells[J]. ACS applied materials & interfaces, 2015, 7(27): 14690-14698.

[38] Hahn H, Schulze H. Über ternäre Selenide des Bariums[J]. Naturwissenschaften, 1965, 52(14): 426-426.

[39] Guen L, Glaunsinger W S, Wold A. Physical properties of the quarternary chalcogenides Cu2IBIICIVX4 (BII= Zn, Mn, Fe, Co; CIV= Si, Ge, Sn; X= S, Se)[J]. Materials Research Bulletin, 1979, 14(4): 463-467.

[40] Altosaar M, Raudoja J, Timmo K, et al. Photovoltaic Energy Conversion, IEEE 4th World Conf[J]. Ser.(Waikoloa, HI), 2006 (148).

[41] Babu G S, Kumar Y B K, Bhaskar P U, et al. Effect of post-deposition annealing on the growth of $Cu_2ZnSnSe_4$ thin films for a solar cell absorber layer[J]. Semiconductor Science and Technology, 2008, 23(8): 085023.

[42] Zhang H, Ma X, Yang D. Effects of complexing agent on CdS thin films prepared by chemical bath deposition[J]. Materials Letters, 2004, 58(1): 5-9.

[43] Roy P, Srivastava S K. A new approach towards the growth of cadmium sulphide thin film by CBD method and its characterization[J]. Materials chemistry and physics, 2006, 95(2): 235-241.

[44] S.G. Mokrushin, Y.D. Tkachev Kolloidn Zh., 23 (1961), p. 438

[45] R.S.Mane, C.Lokhande Chemical deposition method for metal chalcogenide thin films, *Materials Chemistry and Physics 65*, (2000) pp.1-31

[46] Chattarki A N, Kamble S S, Deshmukh L P. Role of pH in aqueous alkaline chemical bath deposition of lead sulfide thin films[J]. Materials Letters, 2012, 67(1): 39-41.

[47] Hariskos D, Powalla M, Chevaldonnet N, et al. Chemical bath deposition of CdS buffer layer: prospects of increasing materials yield and reducing waste[J]. Thin Solid Films, 2001, 387(1): 179-181.

[48] Hodes G. Chemical solution deposition of semiconductor films [M]. CRC press, 2002.

[49] Rahmani S, Shanti R, Morris E. Structural Properties, Density Functional Theory (DFT), Natural Bond Orbital and Energy Calculations for the Fluorous compound: C 18 H 10 F 11 BrN 4 O[J]. Fluorine Notes, 2014, 5(96).

[50] https://en.wikipedia.org/wiki/Raman_spectroscopy

[51] Goldstein J, Newbury D E, Echlin P, et al. Scanning electron microscopy and X-ray microanalysis: a text for biologists, materials scientists, and geologists[M]. Springer Science & Business Media, 2012.

[52] Priambodo P S, Sukoco D, Purnomo W, et al. Electric energy management and engineering in solar cell system[M]//Solar Cells-Research and Application Perspectives. InTech, 2013.

[53] Priambodo P S, Sukoco D, Purnomo W, et al. Electric energy management and engineering in solar cell system[M]//Solar Cells-Research and Application Perspectives. InTech, 2013.

[54] Green M A. Solar cells: operating principles, technology, and system applications[J]. 1982.

[55] Muska K. Study of Composition and Thermal Treatments of Quaternary Compounds for Monograin Layer Solar Cells[M]. TUT Press, 2012.

[56] Mwabora J M. Effect of Recombination on Series Resistance in eta Solar Cell Modified with In(OH)xSy Buffer Layer[J]. 2013.

[57] M. Altosaar, J. Raudoja, K. Timmo, M. Danilson, M. Grossberg, J. Krustok, E. Mellikov, phys. stat. sol. (a) 205 (2008) 167-170.

[58] G. Perna, M. Lastella, M. Ambrico, V. Capozzi, Appl. Phys. A 83(2006) 127-130

[59] H.R. Chandrasekhar, R.G. Humphreys, U. Zwick, M. Cardona, Phys. Rev. B 15 (1977) 2177-2183.

[60] V. V. Poborchii, A.V. Kolobov, K. Tanaka, Appl. Phys. Lett. 72 (1998) 1167-1169.

[61] R.C.C. Leite, S.P.S. Porto, Phys. Rev. Lett. 17 (1966) 10.

[62] Van Wijck M A A M. Atomic layer deposition: U.S. Patent 6,585,823[P]. 2003-7-1.

[63] https://en.wikipedia.org/wiki/Pulsed_laser_deposition.

ACKNOLEDGEMENTS

This thesis is based on the experimental work carried out at the Department of Materials and Environmental Technology, Tallinn University of Technology.

First, I'd like to thank my supervisor, senior research scientist Dr. Mare.Altosaar, she is always very patient with my questions both from theoretical knowledge and experimental operation skills, also she gave me lots of suggestions about my thesis work. Second, I'd like to thank my research group members Dr. Liina Reichmann (co-supervisor), Dr. Tiit Varema, Dr. Jaan Raudoja, Maris Pilvet, Dr. Kristi Timmo, Dr. Marit Kauk-Kuusik, they also gave me lots of support in my experimental work. Then, I'd like to thank other stuff who taught me some operational skills of physical analysis, they are Dr. Valdek Mikli, Dr. Sergei Bereznev, Rainer Traksmaa, Dr. Taavi Raadik and Dr. Maarja Grossberg.

Last, I want to thank my family, their support let me to finish my master thesis and I would like to thank lots of friends both from my home country and here, in Estonia, they gave me a lot of spiritual help.